Monthly Notices
of the
ROYAL ASTRONOMICAL SOCIETY

Mon. Not. R. Astron. Soc. **399,** 2107–2128 (2009) doi:10.1111/j.1365-2966.2009.15408.x

Cosmological systematics beyond nuisance parameters: form-filling functions

T. D. Kitching,[1,2⋆] A. Amara,[3] F. B. Abdalla,[4] B. Joachimi[5] and A. Refregier[6]

[1]*University of Oxford, Department of Physics, Keble Road, Oxford OX1 3RH*
[2]*SUPA, University of Edinburgh, Institute for Astronomy, Royal Observatory Edinburgh, Blackford Hill, Edinburgh EH9 3HJ*
[3]*Department of Physics, ETH Zurich, Wolfgang-Pauli-Strasse 16, CH-8093 Zurich, Switzerland*
[4]*Department of Physics and Astronomy, University College London, Gower Street, London WC1E 6BT*
[5]*Argelander-Institut fur Astronomie (AIfA), Universitat Bonn, Auf dem Hugel 71, 53121 Bonn, Germany*
[6]*Service d'Astrophysique, CEA Saclay, Batiment 709, 91191 Gif-sur-Yvette Cedex, France*

Accepted 2009 July 16. Received 2009 July 14; in original form 2008 December 9

ABSTRACT

In the absence of any compelling physical model, cosmological systematics are often misrepresented as statistical effects and the approach of marginalizing over extra nuisance systematic parameters is used to gauge the effect of the systematic. In this article, we argue that such an approach is risky at best since the key choice of function can have a large effect on the resultant cosmological errors.

As an alternative we present a functional form-filling technique in which an unknown, residual, systematic is treated as such. Since the underlying function is unknown, we evaluate the effect of every functional form allowed by the information available (either a hard boundary or some data). Using a simple toy model, we introduce the formalism of functional form filling. We show that parameter errors can be dramatically affected by the choice of function in the case of marginalizing over a systematic, but that in contrast the functional form-filling approach is independent of the choice of basis set.

We then apply the technique to cosmic shear shape measurement systematics and show that a shear calibration bias of $|m(z)| \lesssim 10^{-3}\,(1+z)^{0.7}$ is required for a future all-sky photometric survey to yield unbiased cosmological parameter constraints to per cent accuracy.

A module associated with the work in this paper is available through the open source ICOSMO code available at http://www.icosmo.org.

Key words: methods: data analysis – methods: numerical – methods: statistical – cosmology: observations.

1 INTRODUCTION

Cosmology is entering a formative and crucial stage, from a mode in which data sets have been relatively small and the statistical accuracy required on parameters was relatively low, into a regime in which the data sets will be orders of magnitude larger and the statistical errors required to reveal new physics (e.g. modified gravity – Heavens, Kitching & Verde 2007; Kunz & Sapone 2007; massive neutrinos – Cooray 1999; Abazajian & Dodelson 2003; Hannestad & Wong 2007; Kitching et al. 2008c; dark energy – Albrecht et al. 2006; Peacock & Schneider 2006) are smaller than any demanded thus far. The ability of future experiments to constrain cosmological parameters will not be limited by the statistical power of the probes used but, most likely, by systematic effects that will be present in the data, and that are inherent to the methods themselves.

The problem that we will address is how the final level of systematics, at the cosmological parameter estimation stage, should be treated. This problem is of relevance to all cosmological probes, some examples include weak lensing and intrinsic alignments (Crittenden et al. 2000; Heavens, Refregier & Heymans 2000; Catelan, Kamionkowski & Blandford 2001; Brown et al. 2002; Heymans & Heavens 2003; King & Schneider 2003; Hirata & Seljak 2004; Bridle & Abdalla 2007; Bridle & King 2007), baryon oscillations and bias (e.g. Seo & Eisenstein 2003), X-ray cluster masses and the mass–temperature relation (e.g. Pedersen & Dahle 2007) to name a few.

The general thesis we advocate in this article is that the standard approach to systematics that of assuming some parametrization and fitting the extra parameters simultaneously to cosmological parameters (e.g. Kitching, Taylor & Heavens 2008a; Bridle & King 2007;

⋆E-mail: tdk@astro.ox.ac.uk

Huterer et al. 2006; for weak lensing analyses) both misrepresent a systematic effect as a statistical signal and more importantly is not robust to the choice of parametrization.

As an alternative, we will present a method, 'form-filling functions', in which a systematic is treated as such: an unknown function which is present in the data. By exhaustively exploring the space of functions allowed by either data, simulations or theory, the effect of a systematic on cosmological parameter estimation – a bias in the maximum likelihood – can be fully characterized. This is a natural extension of the work presented in Amara & Refregier (2008). We will present this using a simple toy model to explain and demonstrate the essential aspects of the formalism. We will then apply this technique to the problem of shape measurement systematics in weak lensing.

We begin in Section 2 by categorizing the different approaches to systematics that can be taken, Section 3 introduces the parameter estimation formalism and how systematics can be included in a number of alternative ways. We will then introduce a toy model that will then be used to introduce 'form-filling functions' in Section 4 where we will also compare the standard approach to systematics to the one taken here. The application to weak lensing shape measurement systematics is presented in Section 5 and conclusions will be discussed in Section 6.

2 APPROACHES TO SYSTEMATIC EFFECTS

In this section, we will discuss the problems that may be faced with respect to systematics and also address the possible ways that these problems can be addressed.

There are two scenarios in which systematic questions may arise. Either some data are available, from which information must be extracted, and the effect of systematics on some parameters measured must be addressed, or one is planning for a future experiment and the potential impact of systematics on some interesting parameters must be forecasted. In both cases, there may be some extra data available that have partially measured the systematic effect, or there may be some hard boundary within which it is known that the systematic must lie – either from a theory or from simulation. When forecasting one may want to place a constraint on the quality of the extra data needed, or the extent of the hard boundary such that future measurements are robust. For both data fitting and forecasting, there are a number of methods that can be employed to address the systematics which we review here.

In the following we will consider a generic method for which the data are an observed correlation (covariance) $C^{\rm obs}$ which is a sum of a 'signal' $C^{\rm signal}(\boldsymbol{\theta})$, which depends on a set of statistical (cosmological) parameters $\boldsymbol{\theta}$, and a general additive systematic effect $C^{\rm sys}$ (that can, or cannot, depend on the parameters we wish to measure), so that the total observed signal is now

$$C^{\rm obs}(\boldsymbol{\theta}) = C^{\rm signal}(\boldsymbol{\theta}) + C^{\rm sys}(\boldsymbol{\theta}) + C^{\rm noise}(\boldsymbol{\theta}). \quad (1)$$

We have also added a benign shot-noise term $C^{\rm noise}$ [which again can, or cannot, depend on the parameter(s) being measured]. We do not claim that all systematics can be written this way (but most can when the data used are a correlation/covariance of quantities) – a multiplicative bias is just a special kind of additive term which has the same form as the signal but is multiplied by a systematic constant.

We have identified three broad categories of approach that could be taken when dealing with systematics.

2.1 Marginalization

Marginalization of systematics entails using a model, a function containing a set of parameters $\boldsymbol{a}$, to characterize the systematic effect $C^{\rm sys} \rightarrow {\rm C}^{\rm sys}(\boldsymbol{a})$. In this case, the cosmological parameters $\boldsymbol{\theta}$ *and* the systematic parameters $\boldsymbol{a}$ are measured simultaneously. The extra 'nuisance' parameter errors are marginalized over to arrive at the final cosmological parameter errors that now take into account the systematic.

Marginalization misinterprets the systematic as a statistical signal (attempts to characterize the systematic by finding best-fitting parameters), by reducing the estimation and determination of the systematic into a parameter estimation problem. It would be an inappropriate statistical approach to estimate nuisance parameters that were known to have a very small degeneracy with cosmological parameters and then to claim that systematics were negligible.

When marginalizing, one is immediately faced with the choice of model. In the absence of some underlying physical theory, one is forced to parametrize. The key choice of parametrization is what makes this approach risky (at best); both the number of parameters and the prior (if any) on those parameters can dramatically affect the level of influence that the systematic may have on cosmological parameter estimation. One can choose either simple models, whose small degree of freedom may have a minimal impact on the cosmological parameters, but whose behaviour may mask the true systematic signal, or very flexible models; but one is always limited by the number of degrees of freedom that can be estimated from the data, and using, for example, $\gg$100 nuisance parameters to find the systematic error on $\sim$10 cosmological parameters seems asymmetric.

In some circumstances, there are physical models that can be called upon to model a systematic accurately, in this case marginalization becomes an attractive option. One could also use more sophisticated techniques, such as Bayesian evidence, to determine which parametrization is warranted given the data available. But even in such a scenario the question of whether an *even more* apt model is available, or not, would always remain and even in this case a *residual* systematic will remain (at least due to noise) which may contain a still unknown effect and must be treated in the correct way.

2.2 Bias formalism

The systematic is not marginalized over in cosmological parameter estimation, but is left in as a systematic term $C^{\rm sys} \neq C^{\rm sys}(\boldsymbol{\theta})$. By 'leaving a systematic in' and not marginalizing over parameters the systematic is correctly identified as a systematic effect, albeit that the magnitude of the effect must be correctly quantified. If a systematic is 'left in', then the cosmological parameter errors themselves are unaffected (in the case that the observation is not dominated by the systematic). The maximum-likelihood value of the cosmological parameters however will always be biased by an amount which depends upon the true, underlying, systematic signal. There have been studies of the biases that can be caused when a systematic is treated as such (e.g. Huterer & Takada 2005; Amara & Refregier 2008; Kitching et al. 2008a), although all studies have assumed some functional form for the underlying systematic.

The task is then to investigate all possible functional forms for the systematic that are allowed by either theory or data so quantifying the extent of the possible biases. In this case, flexibility is paramount since every possible allowed function must be tested. This is the approach advocated in this article.

By treating the systematic in this way, as a true systematic effect as opposed to a statistical effect (as in marginalization), we can move away from the dilemma of choosing a particular parametrization.

2.3 Nulling

The general approach to nulling is that the statistical signal used (the way in which the data are used to extract cosmological information) can be modified in such a way that the systematic signal is cancelled out, i.e. $C^{\rm obs} = C^{\rm signal} + C^{\rm sys} + C^{\rm noise} \rightarrow C^{\rm obs}_{\rm new} = C^{\rm signal}_{\rm new} + C^{\rm noise}_{\rm new}$ and $C^{\rm sys}_{\rm new} = 0$. Cosmological parameter estimates can then be made using this new statistic which by construction has minimized, or completely removed, the systematic effect.

The nulling approach is a potentially powerful tool, for example as shown by Joachimi & Schneider (2008) this could be used in the removal of weak lensing intrinsic alignment contaminant. However when nulling, the cosmological signal is changed in such a way that parameter constraints can be severely degraded. We will not address the nulling approach further in this article, but note that the possibility of 'optimal' weighting (partial nulling) should exist, in a mean-square error (MSE) sense. Nulling aims to set the bias due to a systematic to zero, which may be to strict since our true requirement is simply that the biases are subdominant to the statistical errors.

In the next section, we will review the marginalization procedure and formalize the biasing effect of leaving a systematic in the signal. What we endorse within the context of the bias formalism is using the theory and data themselves to investigate the full range of allowed functions, thus fully characterizing the effect that a systematic may have.

3 THE GENERAL FORMALISM

A common approach in cosmology is to measure the signal of some quantity, and match this to the theory in order to constrain cosmological parameters. However, as we will show, the effect of systematics on such cosmological probes is usually dealt with in a way which can potentially mask their true impact.

Fig. 1 shows the basic situation which we will address. The left-hand panel shows the observable $C^{\rm obs}$ which is a sum of the signal $C^{\rm signal}$ and some systematic plus noise $C^{\rm sys} + C^{\rm noise}$ (equation 1). Furthermore, there is some tolerance envelope around the systematic (grey solid lines) which represents the state of knowledge regarding the systematic. One can then subtract the mean $C^{\rm sys}$ and $C^{\rm noise}$ from the observable which results in an estimator of the signal $\widehat{C^{\rm signal}}$

$$C^{\rm obs} - \langle C^{\rm sys}\rangle - \langle C^{\rm noise}\rangle = \widehat{C^{\rm signal}} + \widetilde{C^{\rm sys}} \tag{2}$$

plus some residual systematic $\widetilde{C^{\rm sys}}$ which is centred around zero. In general, throughout we always consider the case that there are some extra data that place constraints on the systematic $\widetilde{C^{\rm sys}}$. This is shown in the right-hand panel of Fig. 1, the systematic tolerance envelope now lies about the $C(x) = 0$ line.

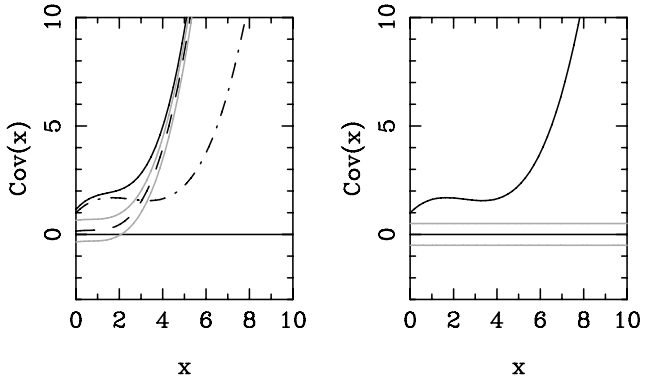

Figure 1. An example of the basic premise concerning the parameter estimation methodology. The left-hand panel shows a total observed correlation (solid black line), that is a sum of the signal (dot–dashed line) and systematic plus noise (dashed line). The systematic is known to lie within some tolerance envelope (within the grey solid lines). The right-hand panel shows the observation minus the mean of the systematic plus noise, leaving an estimator of the signal (solid line) and a systematic tolerance about zero.

The measurement of this signal to estimate the values of some parameters $\boldsymbol{\theta}$ within a theory $C^{\rm signal}_{\rm theory}(\boldsymbol{\theta})$ can be done in the usual way

$$\chi^2(\boldsymbol{\theta}) = \sum_x \sigma_C^{-2}\left[\widehat{C^{\rm signal}} - C^{\rm signal}_{\rm theory}(\boldsymbol{\theta})\right]^2, \tag{3}$$

where $\sigma_C(x)$ is the error on the signal. Note that we will remove (x) [e.g. $\sigma_C(x) \rightarrow \sigma_{\rm C}$] from all equations for clarity. A best estimator of the parameters from the observation $\hat{\boldsymbol{\theta}}$ is defined such that $\mathrm{d}\chi^2/\mathrm{d}\boldsymbol{\theta} = 0$. However, this statistic has not taken into account the residual systematic effect in any way.

To make predictive statements regarding parameter estimation, it is convenient to work with the Fisher matrix formalism. The Fisher matrix allows for the prediction of parameter errors given a specific experimental design and method for extracting parameters. In the case of Gaussian-distributed data where we assume that the error on the signal is not a function of parameter values $\sigma_C \neq \sigma_C(\boldsymbol{\theta})$, we can take the covariance of the estimated values of the parameters (Jungman et al. 1996; Tegmark, Taylor & Heavens 1997; Fisher 1935)

$$\mathrm{cov}[\hat{\boldsymbol{\theta}}_i, \hat{\boldsymbol{\theta}}_j] = \langle(\hat{\boldsymbol{\theta}}_i - \langle\hat{\boldsymbol{\theta}}_i\rangle)(\hat{\boldsymbol{\theta}}_j - \langle\hat{\boldsymbol{\theta}}_j\rangle)\rangle = F^{-1}_{ij}, \tag{4}$$

where the Fisher matrix is defined by (Tegmark et al. 1997; Jungman et al. 1996; Fisher 1935)

$$F_{ij} = \sum_x \left(\sigma_C^{-2}\frac{\partial C}{\partial \boldsymbol{\theta}_i}\frac{\partial C}{\partial \boldsymbol{\theta}_j}\right). \tag{5}$$

The marginal errors on the parameters are given by $\Delta\theta_i = \sqrt{(F^{-1})_{ii}}$, this is the minimum marginal error that one can expect for the experimental design considered (due to the Cramer–Rao inequality; Tegmark et al. 1997).

3.1 Model fitting and marginalization

The marginalization approach fits a model to the residual systematic and treats the systematic as an extra statistical effect. The model chosen for the systematic $C^{\rm sys}_{\rm theory}(\boldsymbol{a})$ depends on a suite of new parameters $\boldsymbol{a}$ and on the original parameter set $\boldsymbol{\theta}$ where the total parameter set is given by $\boldsymbol{\Phi} = (\boldsymbol{\theta}, \boldsymbol{a})$. The extra parameters are then assumed to be part of the signal of a method. To estimate the values of the parameters $\boldsymbol{\theta}$, the χ^2 statistic of equation (3) is modified to

$$\begin{aligned}\chi^2_{\rm total}(\boldsymbol{\theta}, \boldsymbol{a}) &= \sum_x \sigma^{-2}_{C^{\rm signal}}\left[\widehat{C^{\rm signal}} - C^{\rm signal}_{\rm theory}(\boldsymbol{\theta}) - C^{\rm sys}_{\rm theory}(\boldsymbol{a})\right]^2 \\ &\quad + \sum_x \sigma^{-2}_{C^{\rm sys}}\left[\widetilde{C^{\rm sys}} - C^{\rm sys}_{\rm theory}(\boldsymbol{a})\right]^2,\end{aligned} \tag{6}$$

where the total χ^2 is minimized to find the best estimator of the parameters. The likelihood functions for the cosmological parameters

are found by marginalizing the combined likelihood $p(\boldsymbol{\theta}, \boldsymbol{a})$ over the new parameters

$$p(\boldsymbol{\theta}) = \int \mathrm{d}\boldsymbol{a}\, p(\boldsymbol{\theta}, \boldsymbol{a}). \tag{7}$$

The new Fisher matrix for the total parameter set $\boldsymbol{\Phi}$ becomes a combination of the cosmological Fisher matrix $F^{\boldsymbol{\theta\theta}}$, the derivatives of the likelihood with respect to the cosmological parameters and the systematic parameters $F^{\boldsymbol{\theta a}}$ and the systematic parameters with themselves $F^{\boldsymbol{aa}}$

$$F^{\boldsymbol{\Phi\Phi}} = \begin{pmatrix} F^{\boldsymbol{\theta\theta}} & F^{\boldsymbol{\theta a}} \\ F^{\boldsymbol{a\theta}} & F^{\boldsymbol{aa}} \end{pmatrix}, \tag{8}$$

where the individual terms are given by

$$\begin{aligned} F_{ij}^{\boldsymbol{\theta\theta}} &= \sum_x \left(\sigma_{C^{\rm signal}}^{-2} \frac{\partial C_{\rm theory}^{\rm signal}}{\partial \boldsymbol{\theta}_i} \frac{\partial C_{\rm theory}^{\rm signal}}{\partial \boldsymbol{\theta}_j} \right), \\ F_{ij}^{\boldsymbol{\theta a}} &= \sum_x \left(\sigma_{C^{\rm signal}}^{-2} \frac{\partial C_{\rm theory}^{\rm signal}}{\partial \boldsymbol{\theta}_i} \frac{\partial C_{\rm theory}^{\rm signal}}{\partial \boldsymbol{a}_j} \right), \\ F_{ij}^{\boldsymbol{aa}} &= \sum_x \left(\sigma_{C^{\rm signal}}^{-2} \frac{\partial C_{\rm theory}^{\rm sys}}{\partial \boldsymbol{a}_i} \frac{\partial C_{\rm theory}^{\rm sys}}{\partial \boldsymbol{a}_j} \right) \\ &\quad + \sum_x \left(\sigma_{C^{\rm sys}}^{-2} \frac{\partial C_{\rm theory}^{\rm sys}}{\partial \boldsymbol{a}_i} \frac{\partial C_{\rm theory}^{\rm sys}}{\partial \boldsymbol{a}_j} \right), \end{aligned} \tag{9}$$

where we have assumed that the errors are uncorrelated and do not depend on the parameters.

The predicted cosmological parameter errors now including the effect of the systematic are given by $\Delta\theta_i = \sqrt{[(F^{\boldsymbol{\Phi\Phi}})^{-1}]_{ii}}$ (see Appendix A for a more detailed expression). The cosmological parameter errors are increased due to the degeneracy between the cosmological and systematic parameters (included by the $F^{\boldsymbol{\theta a}}$ terms). The tolerance envelope around the residual systematic (Fig. 1) acts as a prior on the systematic parameters in the chosen model.

3.2 The bias formalism

The bias formalism treats a systematic as such, by not statistically marginalizing over any extra parameters within a model. Instead, the systematic simply adds an extra systematic function to the signal. By doing this, a bias is introduced in the maximum-likelihood value of the parameters with respect to the true underlying values

$$b[\boldsymbol{\theta}_i] = \langle \hat{\boldsymbol{\theta}}_i \rangle - \left\langle \hat{\boldsymbol{\theta}}_i^{\rm true} \right\rangle. \tag{10}$$

When marginalizing, the choice lies in the suite of parameters, and the function, chosen. Here there is a similar choice, one must assume that the systematic has some functional form $C_{\rm function}^{\rm sys}$. To estimate the values of the cosmological parameters $\boldsymbol{\theta}$, the χ^2 statistic of equation (3) is modified to include the assumed systematic

$$\chi^2(\boldsymbol{\theta}) = \sum_x \sigma_C^{-2} \left[\widehat{C^{\rm signal}} + C_{\rm function}^{\rm sys} - C_{\rm theory}^{\rm signal}(\boldsymbol{\theta}) \right]^2. \tag{11}$$

The estimate of the parameter values will now be biased but the marginal error on the parameters will remain the same (the caveat here that this is only the case when the systematic is smaller than the signal).

It can be shown (Kim et al. 2004; Taylor et al. 2007; Amara & Refregier 2008) that, with the assumption of Gaussian likelihoods, the predicted bias in a parameter due to an uncorrected systematic is given by

$$b(\boldsymbol{\theta}_i) = (F^{-1})_{ij} B_j, \tag{12}$$

where

$$\begin{aligned} F_{ij} = F_{ij}^{\boldsymbol{\theta\theta}} &= \sum_x \left(\sigma_C^{-2} \frac{\partial C_{\rm theory}^{\rm signal}}{\partial \boldsymbol{\theta}_i} \frac{\partial C_{\rm theory}^{\rm signal}}{\partial \boldsymbol{\theta}_j} \right), \\ B_j &= \sum_x \sigma_C^{-2} C_{\rm function}^{\rm sys} \frac{\partial C_{\rm theory}^{signal}}{\partial \boldsymbol{\theta}_j}. \end{aligned} \tag{13}$$

To recap Sections 2 and 3, Table 1 summarizes the effect on the likelihood surface and the primary problem encountered by each systematic approach.

In cases where the systematic affects the error on the signal $\sigma_C = \sigma_C(C^{\rm sys})$ (which is almost always) then leaving a systematic in the signal can cause a bias and increase the marginal errors. However, the increase in marginal errors is negligible for systematics that have an amplitude which is much less than the signal, and cause biases that are $\lesssim 10\sigma$ (Amara & Refregier 2007). Equation (12) is also an approximation for the case of small biases, if the bias is large relative to the marginal error then the curvature of the likelihood surface will have varied substantially from the Gaussian approximation. In such cases, one could go to a higher order in the Taylor expansion used to derive equation (12), or calculate the full likelihood.

3.3 A simple example

To review the general formalism described thus far, and for use in subsequent sections, we will here introduce a simple model. The toy model we will consider is shown in the right-hand panel of Fig. 1. Referring to equation (1), the signal is given by a simple polynomial expansion

$$C_{\rm example}^{\rm signal}(x) = a_0 + a_1 x + (-0.45)x^2 + (0.05)x^3, \tag{14}$$

where the statistical parameters we are concerned with (with fiducial, true, values) are the parameters $a_0 = 1.0$ and $a_1 = 1.0$. We assume that the observed signal is measured with an error of $\sigma_C(x) = 0.25$. We include the x^2 and x^3 terms so that the problem is slightly more realistic, in that there is an extra behaviour in the signal that we do not wish to constrain but may effect the determination of the parameters of interest.

Fig. 2 shows the simple model signal with some Gaussian-distributed data points. We then calculate the two-parameter marginal errors using equation (3) where we use the model as in equation (14). Table 2 shows the measured marginal errors from this simple mock data, and compares these with the expected marginal errors calculated using the Fisher matrix (equation 5).

Table 1. A summary of the different approaches to systematic effects, showing the effect on the likelihood surface and the primary problem that each method encounters.

Approach	Broadens likelihood	Bias likelihood	Problems
Marginalize	$\surd$	$\times$	Choice of parametrization
Bias formalism	$\times^{\dagger}$	$\surd$	Need to assess all allowed functions

†Only in the case that the systematic is subdominant to the signal.

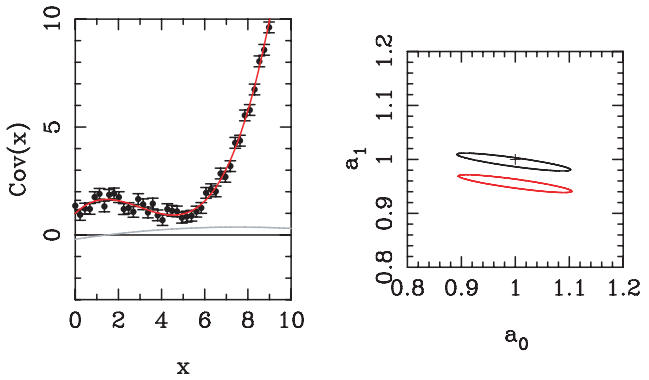

Figure 2. The left-hand panel shows the toy model signal, the fiducial model is shown in red (dark grey) and we have added some simple Gaussian-distributed data points about this central model. We also show an example systematic in (light) grey defined in equation (15). The right-hand panel shows the two-parameter 1σ error contours without a systematic (black) and including the example systematic (red/dark grey). The fiducial model is marked by $+$.

Table 2. This table compares the Fisher matrix predictions with values found using some simple mock data described in Section 3.3. This is not a comparison of the systematic methods themselves, which will be done in Section 4.3.

No Systematics		
Parameter	Measured error	Expected error
a_0	0.100	0.099
a_1	0.011	0.011
Bias method		
Parameter	Measured bias	Expected bias
a_0	0.003	0.002
a_1	0.040	0.040
Marginalizing method		
Parameter	Measured error	Expected error
a_0	0.120	0.119
a_1	0.012	0.013

Note. The upper table shows the marginal errors found using the data shown in Fig. 2 for the parameters a_0 and a_1 defined in equation (14). These errors are compared to what is expected from the Fisher matrix (equation 5). The middle table shows the measured bias when a simple systematic is added (equation 15) and compares this to the expected bias calculated using equation (12). The lower table shows the increased marginalized errors on a_0 and a_1 when a simple parametrized systematic model is marginalized over.

We then introduce a simple systematic into the model by assuming a simple function [note that this does not have a mean of zero, but could fit into some boundary centred on $C(x) = 0$]

$$C^{\rm sys}_{\rm example}(x) = -0.2 + 0.15x - 0.01x^2. \quad (15)$$

By recalculating the likelihood and including this systematic function, using equation (11), we find that the most likely value of a_0 and a_1 is biased and yet the marginal errors remain the same. We compare this bias to the prediction made using equation (12) in Table 2.

To test the method of marginalizing over data, we now reset the systematic (throw away equation 15) and introduce a simple systematic which is measured using some mock data. Fig. 3 shows the model signal with some extra systematic data with a mean of zero and a scatter of $\sigma_{C^{\rm sys}} = 0.5$. We then introduce a simple systematic

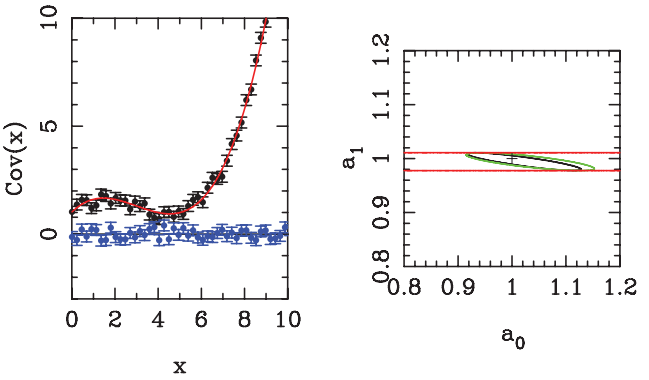

Figure 3. The left-hand panel shows the model signal, the fiducial model is shown in red (dark grey) and we have added some Gaussian-distributed data points about this central model. We also show an example data-driven systematic blue (light grey) points about $C(x) = 0$ with a variance of $\sigma_{C^{\rm sys}} = 0.5$. The right-hand panel shows the two-parameter 1σ error contours with (green/light grey) and without (black) marginalizing over the systematic model. The red lines show the marginal error with no extra systematic data, a complete degeneracy between a_0 and s_0. The fiducial model is marked by $+$.

model parametrized by a new parameter s_0

$$C^{\rm sys}_{\rm theory\,example}(x) = s_0 \quad (16)$$

and fit the model (equation 14) and the systematic to the data simultaneously, as described in equation (6). The total likelihood $p(a_0, a_1, s_0)$ is then marginalized over s_0. Fig. 3 shows that when this extra systematic is marginalized over the constraint on a_0 it is affected the most since s_0 has the same functional form as this parameter, and so there exists a large degeneracy between a_0 and s_0. The exact degeneracy is broken by the extra data available for the systematic. In Table 2, we show the increase in the marginal error on the parameters a_0 and a_1 when we marginalize over the extra systematic parameter s_0.

We have now introduced the basic formalism and shown that this can be applied to a simple example that yields results which are in good agreement with the Fisher matrix predictions.

4 FORM-FILLING FUNCTIONS

For the remainder of this article, we will present an alternative to marginalization by advocating the bias formalism for dealing with systematics, outlined in Section 3.2. The issue with which one is now faced is what function to choose for the residual systematic. To investigate the full extent of possible biases, allowed by the tolerance on the systematic, all allowed functions must be addressed in some way.

In Fig. 4, we use an extension of the simple model, outlined in Section 3.3, to introduce the concept of two different forms of systematic tolerance. The tolerance envelope could have a *hard boundary* (e.g. defined by a theory which states that 'the systematic *must* lie within this boundary'), or the systematic could be defined by some extra data that have partially measured the magnitude of the systematic. We will refer to these two scenarios as the 'hard bound' and 'data bound', respectively.

To fully assess the level of bias, every functional form allowed by the systematic tolerance envelope needs to be tested. For the hard boundary, we want to find every function that can be drawn within the hard boundary. For the data bound, every function can be weighted with respect to the data themselves. Here, we introduce

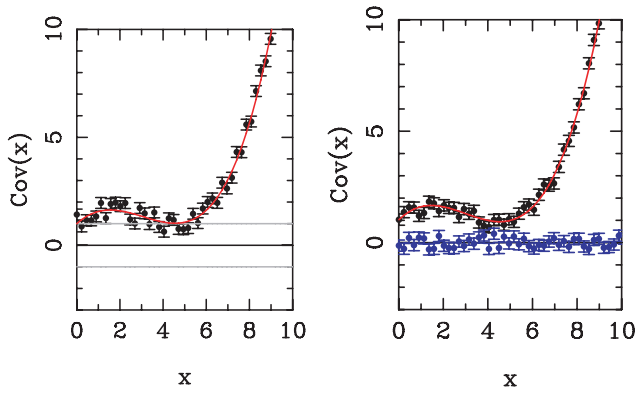

Figure 4. Representing the two possible systematic constraints, either from theory or from data. A hard boundary (left-hand panel; solid grey lines) may be defined within which the systematic must lie, or some data may provide a measurement of the level of systematic (right-hand panel; blue/light-grey error bars). The black data points are mock data with a Gaussian distribution using the model described in Section 3.3, the red (dark grey) line is the fiducial model.

the concept of 'form-filling functions' which is a set of functions that should exhaustively fill the space of possible functions allowed by some tolerance envelope.

Consider the hard bound in Fig. 4, in the bias approach we want to find every function that will fit within this tolerance envelope. To do this, we consider functions in the most general form as expansions in some arbitrary basis set

$$f(x;\{a_n\},\{b_n\}) = \sum_{n=1}^{N} a_n\psi_n(x) + b_n\phi_n(x), \tag{17}$$

where a_n, $b_n \in \Re$ and $\psi_n(x)$ and $\phi_n(x)$ form some arbitrary basis functions. To choose the basis set, we impose the following conditions.

(i) The basis set must be *complete* in the range of x we are considering, i.e. all functions $f(x)$ must be expressible as an expansion in the basis.

(ii) The basis functions must be orthogonal.

(iii) The functions must be *boundable*, i.e. the basis set must be able to be manipulated such that every function described within some bounded region (tolerance envelope) can be drawn.

The first condition is necessary. The second condition is to make some calculations more straightforward though is not strictly necessary. The third condition is merely desirable – one can imagine having a basis set in which non-bounded functions are allowed, but when using such expansions one would have remove these stray functions. As an aside, we note that overcompleteness is not a problem as long as the basis set is in fact complete (we do not care if we sample a function multiple times, as long as we sample it at least once).[1]

Algorithm. Equation (17) represents *every* function, however we are only concerned here with defining all functions within some bounded region. To begin we will show how an interval $|a_n| \leq Q$ can be defined such that every function between $|f(x)| \leq 1$ can be drawn. For an orthonormal basis set, the coefficients needed to draw a function $f(x)$ can be expressed as

$$a_n = A_{nm}\int_R \mathrm{d}x\, w(x) f(x)\phi_{\rm m}(x), \tag{18}$$

where R is some interval over which the basis set is complete and $w(x)$ is a weight function upon which the basis set is complete the constant A (A_{mn} is a diagonal) is calculated in general using

$$A^{-1}_{nm} = \int_R \mathrm{d}x\, w(x)\phi_n(x)\phi_{\rm m}(x) \tag{19}$$

for all the basis sets we consider $A_{nm} = A\delta_{nm}$. Now we can write a general expression that provides a limit on a_n. Using the triangle inequality, we can write

$$|a_n| \leq A\int_R \mathrm{d}x |w(x)||\phi_n(x)||f(x)| \tag{20}$$

and given that $|f(x)| \leq 1$ we have an expression for $|a_n|$

$$|a_n| \leq A\int_R \mathrm{d}x |w(x)||\phi_n(x)||f(x)| \leq A\int_R \mathrm{d}x |w(x)||\phi_n(x)| = Q. \tag{21}$$

So using equation (17) and limiting the coefficient values to $|a_n| \leq Q$ (and similarly for b_n), every function with the region $|f(x)| \leq 1$ can be drawn.[2]

We now define an arbitrary 'bound function' $B(x)$ which describes a hard boundary (e.g. in Fig. 4) where at any given point in x the systematic functional form must lie in the region $-B(x) \leq f(x) \leq B(x)$. Equation (17) is simply modified to include this arbitrary boundary

$$f(x;\{a_n\},\{b_n\}) = B(x)\sum_{n}^{N} a_n\psi_n(x) + b_n\phi_n(x). \tag{22}$$

Now, if the basis set is complete, $N = \infty$ and $|a_n| \leq Q$ (similar for b_n), equation (22) represents *every possible* function that can be drawn within the hard bound – and each function could yield a different bias. Note however that this statement says nothing about the *probability* that a particular function will be drawn.

An important caveat to this is that the total set of functions drawn using this algorithm is not bounded, only some subset of the functions is. However, a 'clean' subset of functions with $|f(x)| \leq B(x)$ can easily be drawn by removing any function for which $|f(x)| > B(x)$ at any x.

In practice, where $N < \infty$ the task of drawing all possible functions becomes a numerical/computational problem. For a given basis set, the fundamental quantities that describe each and every function are the coefficients a_n and b_n. The task then is to explore the coefficient parameter space $\{|a_n| \leq Q\}$ in an exhaustive a manner as possible.

As a first attempt, the approach taken in this article is to randomly and uniformly sample the coefficient space $\{a_1,\ldots,a_N\}$ for $|a_n| \leq Q$. The free parameters in this approach, given a basis set, are the maximum order investigated N and the number of random samples in the space $\{a_n\}$ that are chosen. We leave a more sophisticated Monte Carlo formulation of this problem for future work.

[1] Orthogonal basis sets are never overcomplete, so the second condition means we should not be in this situation for our functional form-filling algorithm.

[2] Equation (21) is strictly only true for Riemann integrable functions, however essentially all bounded functions satisfy this constraint – in particular all class C^0 (smooth) functions, and all step functions. Examples of the type of (very peculiar) function that are not Riemann integrable are Dirichlet's function and the Smith–Volterra–Cantor set.

When truncating the series we will be missing some highly oscillatory functions (for the basis sets considered), but we show in Appendix B that one can always make a definitive statement about the fraction of all functional behaviour sampled down to some scale. These free-form functions are regularized by the truncation of the basis set and by the bound function. Throughout the remainder of this section, we use the numerical order and function number investigated in Appendix B.

Basis sets. Throughout we will principally consider three different basis sets. These are as follows.

(i) *Chebyshev* polynomials $T_n(x)$. These functions form a complete basis set for $-1 \leq x \leq 1$, and are bounded by the region $|f(x)| \leq 1$. To map these functions on to an arbitrary x-range, a variable transformation can be applied such that

$$\psi_n(x) = \cos[n \arccos(x)] = T_n\left(\frac{2x - x_{\rm min} - x_{\rm max}}{x_{\rm max} - x_{\rm min}}\right), \tag{23}$$

and $\phi_n(x) \equiv 0$ for all n.

(ii) *Fourier* series. The Fourier series is a complete basis set in the range $-\pi \leq x \leq \pi$ and the functions are bounded in the region $|f(x)| \leq 1$ for the basis set

$$\psi_n(x) = \frac{1}{2}\cos\left[n\left(\frac{\pi x - \pi x_{\rm min}}{x_{\rm max} - x_{\rm min}}\right)\right]$$
$$\phi_n(x) = \frac{1}{2}\sin\left[n\left(\frac{\pi x - \pi x_{\rm min}}{x_{\rm max} - x_{\rm min}}\right)\right]. \tag{24}$$

The cosine and sine of a real number are $|\cos(x)| \leq 1$ and $|\sin(x)| \leq 1$.

(iii) *Top-hat* functions (binning). This uses a top-hat functional form and is meant to be analogous to binning the x-range. The maximum order in equation (17) N here refers to the number of bins where for the $n^{\rm th}$ bin $\psi(x)$ is either zero or one depending on whether x lies within the bin

$$\psi_n(x) = \begin{cases} 1 & \forall (x_n - \Delta x/2) \leq x \leq (x_n + \Delta x/2) \\ 0 & \end{cases}$$
$$= H\left(x - \frac{\Delta x}{2}\right) - H\left(x + \frac{\Delta x}{2}\right), \tag{25}$$

where $x_n = x_{\rm min} + (n-1)\Delta x$ and $\Delta x = (x_{\rm max} - x_{\rm min})/(N-1)$ is the bin width. $\phi_n(x) \equiv 0$ for all n.

Table 3 summarizes some of the basis set properties including the coefficient intervals over which a complete (sub)set of functions with $|f(x)| \leq 1$ can be drawn.

One may be concerned that there will always be some x at which a boundary-touching function cannot be drawn. For every finite maximum index N in the sum of equation (22), one can find a value of x in R such that $f(x)$ cannot be 1 at x. The key realization that we stress here is that this is a actually a statement about the scale upon which the space of functions is complete. The larger the maximum order N, the smaller one can find an ϵ with $\psi_n(x \pm \epsilon) = 1$ for some n, i.e. the concern is reduced to an issue of resolution because if $\epsilon \ll s$ then every function complete down to some scale s can be drawn. We show this in Appendix B.

4.1 Hard bound

Fig. 5 shows an example of a hard boundary and a random assortment of functions (a random, uniform, sampling of $\{a_1, \ldots, a_N\}$; and $\{b_1, \ldots, b_N\}$ for the Fourier basis set) for the Chebyshev, Fourier and top-hat basis sets. As the order and number of functions are increased, the functional forms begin to completely fill in the bounded area (hence 'form-filling functions').

It can be seen even at this stage that the top-hat basis set is not efficient at filling the bounded area. This is investigated

Table 3. This table lists some constants and functions associated with the basis sets used in this article, Chebyshev, Fourier and top-hat functions. Some of these constants are defined before and used in equation (21). The coefficient interval is such that for $|a_n| \leq Q$ all function in with $|f(x)| \leq 1$ can be drawn.

Basis set	Basis functions	Orthogonal weight $w(x)$	Orthogonal constant A	Interval R	Coefficient interval Q
Chebyshev	$T_n(x) = \cos(n \arccos(x))$	$(1-x^2)^{-\frac{1}{2}}$	$\frac{1}{\pi}$ for $n = 0$; $\frac{2}{\pi}$ for $n \neq 0$	$[-1, 1]$	1 for $n = 0$; $\frac{4}{\pi}$ for $n \neq 0$
Fourier	$\frac{1}{2}$ for $n = 0$, $\cos(nx)$ & $\sin(nx)$	1	$\frac{1}{\pi}$	$[-\pi, \pi]$	2 for $n = 0$; $\frac{4}{\pi}$ for $n \neq 0$
Top-hat	$H(x-\frac{\Delta x}{2})+H(x+\frac{\Delta x}{2})$	1	1	$[-1, 1]$	1

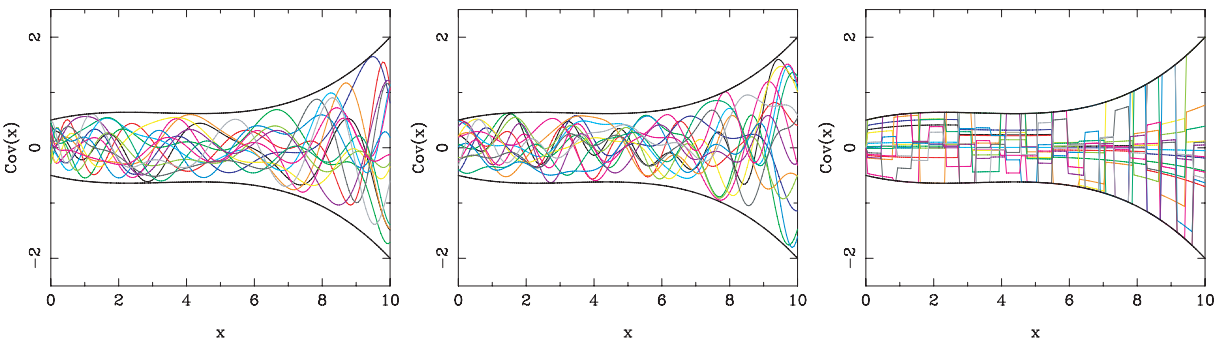

Figure 5. An example of a bounded area (thick black lines), and a random sampling of 15 functions shown by thin coloured (grey and black) lines. Every function is defined, using equation (22) so that it must fit within the bounded area. In the left-hand panel, we used the Chebyshev basis set, in the central panel we use the Fourier basis set and in the right-hand panel we use the top-hat basis set (binning). For all basis sets, the maximum order is $N = 15$. The functions are defined by uniformly and randomly sampling the coefficient space $\{a_1, \ldots, a_{15}\}$. This figure is meant simply as a example of the type of function that can be drawn not as a measure of whether the method succeeds in drawing all functions. The success of the method in drawing all functions is shown in an extensive fashion in Appendix B.

further in Appendix B where we show that whilst all of the basis sets considered can fill any desired bounded region, the Chebyshev and Fourier basis are many orders of magnitude more efficient in terms of computational time than the top-hat functions (binning); we discuss computational time in Appendix C. This is a result of the restrictive step-like nature of the functions that binning imposes requiring a high order (number of bins) to characterize particular (smooth) functional behaviour. In addition to being inefficient, the top-hat basis is not differentiable at the bin boundaries and as such could be construed as being unphysical, although in some special circumstances (e.g. photometric redshifts where a filter may have a top-hat function in wavelength) a top-hat basis set may be needed.

The key feature of the hard bound is that within the boundary all functions are given equal weight, i.e. the probability that any given function is the 'true' systematic functional form is the same for all functions. Out of the full range of possible biases given a hard boundary, there should exist a *maximum bias* – because the space of functions and hence the range of biases is limited. We show that this is the case in Appendix D. The quantity of interest is therefore this maximum bias that is allowed by the functions that can be drawn within the hard boundary. In the data boundary case (Section 4.2), there is a maximum bias for each subset of functions that give the same weight (with respect to the data).

One intuitively expects that the systematic function that introduces the largest bias should be the one that most closely matches the signal term containing each parameter. In the case where there are degeneracies between parameters, the worst function is some combination of the signals sensitivity to the parameters. Here, we will use the simple example hard bound from Section 3.3 to demonstrate that in this case a maximum bias exists, and that this maximum is stable with respect to basis set.

Fig. 6 shows the maximum bias on a_0 as a function of the number of random realizations of the coefficient space for the Chebyshev, Fourier and top-hat systematic basis sets, for all sets we consider a maximum order of 100. It can be seen that as soon as the 'worst function' is found the maximum bias becomes constant and stable for the Chebyshev and Fourier basis sets. In this case, the worst function is simply $C^{\rm sys}(x) = x$ since this is the function that affects the signal $[C^{\rm sig}(x) = a_0 + a_1 x + \text{constant}]$ the most through the effect on a_1 (the worst function is a linear combination of the response of each individual parameter in the marginalized case, see Appendix D). There is an exact degeneracy since a function of the form $-f(x)$ will cause a bias of equal magnitude but opposite sign to $f(x)$, so $C^{\rm sys}(x) = -x$ in this case will also cause the same absolute bias (see Appendix D). For the top-hat basis set, it is very unlikely to find this particular worst function so the bias does not find the maximum even after 100 realizations. The Chebyshev basis set finds this function after only a few realizations since $\psi_1(x) = T_1(x) = x$ is one of the basis functions of the Chebyshev expansion.

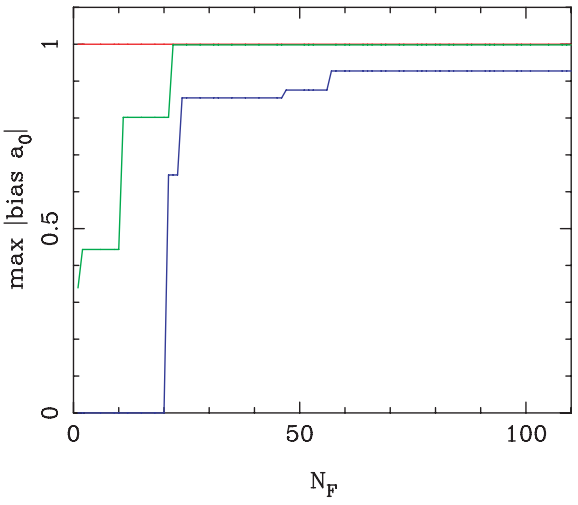

Figure 6. Using the simple example from Section 3.3. The maximum bias on a_0 as a function of the number of realizations of the systematic basis set's coefficients. Red (dark grey, upper line) shows the maximum bias found using the Chebyshev basis set, green (light, middle line) grey shows the maximum bias for the Fourier basis set and blue (darkest grey, lower line) for the top-hat basis set.

Fig. 6 is meant simply as an example of the type of convergence test that could be performed given a realistic application. In Appendix B, we outline a diagnostic mechanism that can gauge whether a bounded area has been completely filled with functions.

4.2 Data bound

If the systematic has been partially measured using data, then there is no hard boundary within which all functions must lie, and every function is still allowed to some degree. The issue which must be addressed in this case is how each function should be weighted given the data available – a function is more likely to be the 'true' systematic signal if it is a good fit to the systematic data.

For the case of a data bound, we propose a similar approach to the hard bound. We want to explore all possible functions, to do this we express an arbitrary function using an expansion as in equation (22). By choosing a complete basis set (e.g. Chebyshev, Fourier), the full space of functions can be explored by exhaustively exploring the space of coefficients, as described in Section 4.1.

In the following, we will concatenate the two basis sets $\{a_n\}$ and $\{b_n\}$ for clarity, however note that for the Fourier basis set two sets of coefficients are needed.

The critical difference in this case is that for each function $f(x;\{a_n\})$ that is drawn we can assign a weight $W(\{a_n\})$ using the χ^2 statistic

$$\chi^2 = \sum_x \frac{[f(x;\{a_n\}) - \widetilde{C^{\rm sys}}]^2}{\sigma^2_{C^{\rm sys}}}. \quad (26)$$

This quantifies how good a fit the function (the values of a_n and b_n, and some basis set) is to the residual systematic data.

However, since we aim to exhaustively try every function (complete down to some scale) there will exist some functions that fit *exactly* through the data points. This causes a problem when using the χ^2 statistic as a weight for such functions will have a $\chi^2 \equiv 0$, and hence be given a probability $P = 1$ that such a function is likely, but such a conclusion has not taken account of the error bars on the systematic data.

In this simple example, we have subtracted the mean of the systematic signal so data should be scattered about $C(x) = 0$. In the case of Gaussian-distributed data, the scatter of the data points should be proportional to the error bar on each data point. If the observation could be repeated, then the data points would be scattered in the same statistical manner about $C(x) = 0$ but have different actual values. This is very similar to the familiar sample variance; in cosmology, we are used to a special kind of sample variance that we call cosmic variance in which the likelihood of the data, given only one realization of our Universe, must be taken into account.

To take into account this sample variance effect, we must consider the likelihood of the residual data. In Appendix E, we show how for Gaussian-distributed data the probability of a function $f(x;\{a_n\})$,

given some set of observations, can be written as a sum over x, where at each point there are some data with an error bar $\sigma_{C^{\rm sys}}$ as

$$\ln p[f(\{a_n\})] \propto -\sum_x \left[\frac{f(x;\{a_n\})^2}{4\sigma^2_{C^{\rm sys}}}\right] + \sum_x \ln(\sigma_{C^{\rm sys}}\sqrt{\pi}), \quad (27)$$

where we have translated the notation of equation (E4) to reflect that of equation (26). For any given set of data, the second term in equation (27) is a benign additive constant so the weight that we assign each function is

$$W(\{a_n\}) = \sum_x \left[\frac{f(x;\{a_n\})^2}{4\sigma^2_{C^{\rm sys}}}\right]. \quad (28)$$

We stress that this is for Gaussian data with a known mean of zero such a function is uniquely described by the variance.

In general, data may not be exactly centred at zero or be Gaussian distributed. As an alternative to the analytic procedure of marginalizing over the data, one could create Monte Carlo realizations. For each realization, one could measure the χ^2 of the fit of a given function to the data from equation (26) and assign a weight as the average over all realizations

$$W(\{a_n\}) = \frac{1}{2}\left\langle \sum_x \frac{\left[f(x;\{a_n\}) - \widetilde{C^{\rm sys}}\right]^2}{\sigma^2_{C^{\rm sys}}} \right\rangle_{\rm realizations}, \quad (29)$$

where the extra factor of $1/2$ converts the average χ^2 to a log-likelihood similar to equation (28).

The bound function in equation (22) represents a hard prior in this case. One should choose a bound function is much larger than the scatter in the systematic data $B(x) \gg \sigma_{\rm sys}(x)$. Any functions that deviate from the data by a large amount will be down-weighted by the poor fit even though they may yield a large bias, so as long as the boundary within which functions are considered is $B(x) > 3\sigma_{\rm sys}(x)$ away from the data then any results should be robust.

For each function $f(x;\{a_n\})$, one now has an associated bias and a weight. Now consider a particular bias in some parameter: there exists a set of systematic functions that could yield this same bias and from that set there must exist a function which is the best fit to the data. If each best-fitting function for every bias can be found, then one is left with a robust weight for each bias and a measure of the relative probability allowed by the data

$$p(b_i) \propto \exp[-\min[W(b_i;\{a_n\})]], \quad (30)$$

where $\min[W(b_i;\{a_n\})]$ is the minimum weight (equation 28) from the space of functions defined by the coefficients $\{a_n\}$ that yields the bias b_i.

Another way of putting this is that for a given weight there exists a maximum and a minimum bias. We show in Appendix D that, within the Fisher matrix approximation of equation (12), there does indeed exist a maximum and minimum bias for each weight.

Fig. 7 shows the weight (equation 28) for each function drawn from the Chebyshev, Fourier and top-hat basis sets against the bias induced by the function using the data bound toy model of Fig. 4. It can be seen from this figure that for any given bias there exists a minimum weight that can be achieved by the functions giving that bias. In the right-bottom panel of Fig. 7, we have found the minimum weight for each bias and converted this into a likelihood using equation (30) showing that this procedure is robust to the choice of basis set used (though the top-hat basis set is far less efficient than Chebyshev and Fourier, see Appendix B for more details).

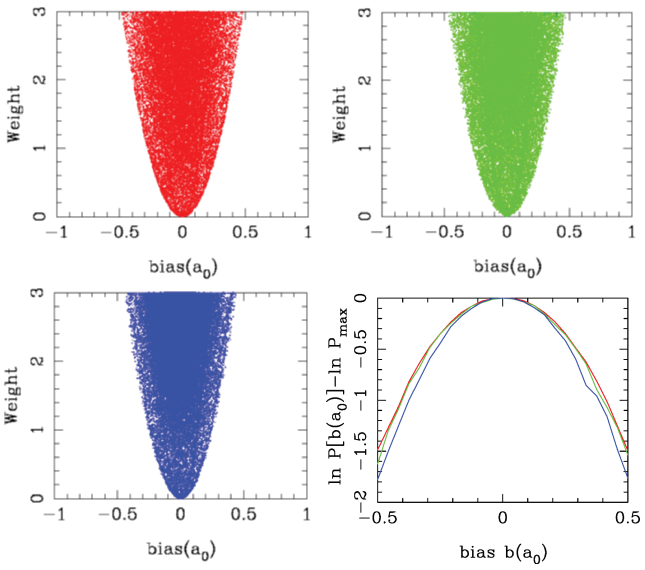

Figure 7. The three scatter plots show the bias in the parameter a_0 caused by fitting functions through the data bounded systematic shown in Fig 4 against the weight given to the function with respect to the systematic data points given in equation (28). Each point represents a function. The colours correspond to the different basis sets considered blue (darkest grey, bottom-left panel) is top-hat functions, red (lighter grey, top-left panel) is Chebyshev functions and green (lightest grey, top-right panel) is Fourier functions. Also shown is the likelihood of the bias in a_0 for each basis set, found by measuring the minimum weight for a particular bias – the lowest extent of the scattered points in the other plots – and using equation (30).

One can of course extend the formalism introduced here to an arbitrary number of dimensions. To extend this to two dimensions, we have modified the simple example to have a much smaller data bound, since (as can be seen in Fig. 7) the fiducial scatter in the toy model systematic data introduces large biases in the measured parameters. Fig. 8 shows the *joint* $1-\sigma$ statistical constraint on a_0 and a_1 for the mock data shown. On this same plot, we show the systematic $1-\sigma$ contours from the residual systematic – within the systematic contour there is a $\geq$68 per cent probability that the statistical maximum likelihood is biased.

We again show results for two different basis sets and show that the systematic contours are again *independent* of the basis set chosen. We have not used the top-hat basis because it is not an efficient basis set (in terms of computational time, see Appendix B) to use even for a one-dimensional analysis.

In a real application, one would hope to show such plots with the systematic contours lying within the statistical ones, but for illustrative purposes we have shown a dominant systematic here. A hard bound in this case would represent a top-hat contour in probability where, within the contour, the probability equals unity and outside the contour the probability is zero.

In the marginalization approach, one could also draw two sets of contours, but both would be statistical: one that has no systematic and the other in which a systematic has been included. Fig. 8 represents one of the key recommendations of this article that in future we must not only show statistical contours for cosmological parameters but also systematic probability contours. Here, we have shown one way of obtaining a robust estimate of such systematic probability contours.

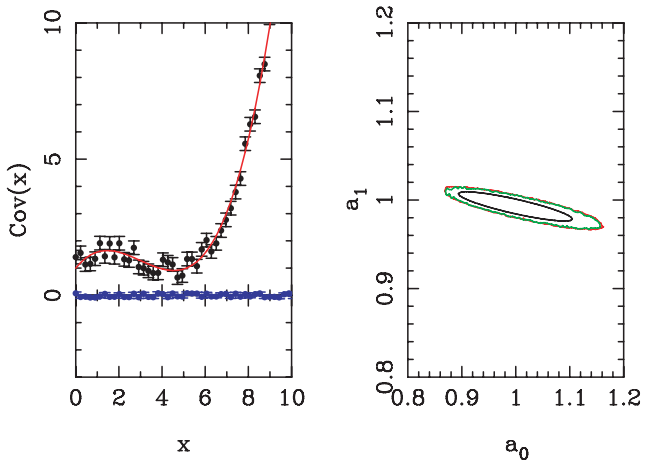

Figure 8. The left-hand panel shows the modified simple example, see Section 3.3, where we have made a more tightly constrained Gaussian residual systematic with $\sigma_{C^{\rm sys}} = 0.05$ for clarity, this can be compared with the right-hand panel in Fig. 4. The right-hand panel shows the 1σ statistical constraints on a_0 and a_1 (black solid line). In addition, we show the *systematic* probability contours for the residual data bound in the left-hand panel. Shown are the 1σ systematic contours using both a Chebyshev (red, dark grey line) and a Fourier (green, light-grey line) basis set for functional form filling.

4.3 Marginalization versus bias

The bias and the marginal error are interrelated via the MSE which is defined, for a parameter a_i, as

$$\mathrm{MSE} = \sigma^2(a_i) + b^2(a_i), \tag{31}$$

where $\sigma(a_i)$ is the marginal error on a_i and $b(a_i)$ is the bias. So both marginalization over systematic parameters and functional form filling increase the MSE through the marginal error and bias, respectively.

In Appendix A, we show that the marginalizing approach and the functional form-filling approach are different; however, there is a subtlety. If the parametrization and order are the same (i.e. a truncated basis set is used), then the MSE recovered from marginalizing or considering the bias is the same. The conclusions from Appendix A are as follows.

(i) If the functional form of the systematic is known, then the degradation in the MSE as a result of marginalizing or functional form filling (bias) is the same.

(ii) If the functional form of the systematic is unknown, then the MSE from marginalizing will tend to underestimate the true systematic error and is in general not equal to the MSE from functional form filling.

(iii) Given that the marginalizing necessarily truncates the basis set, there are always some functions that marginalizing cannot assess.

Given that the MSE, given a particular functional subset, is the same for bias and marginalization the key difference between marginalization and functional form filling is that in the marginalization case the functional space is truncated by the choice of parametrization and ultimately by the number of data points.

Looking back at Fig. 7, the functional form-filling technique fills out the weight–MSE (bias) bounded region by sampling every function down to some scale. To illustrate the way in which marginalization cannot sample the full space of functions, we have

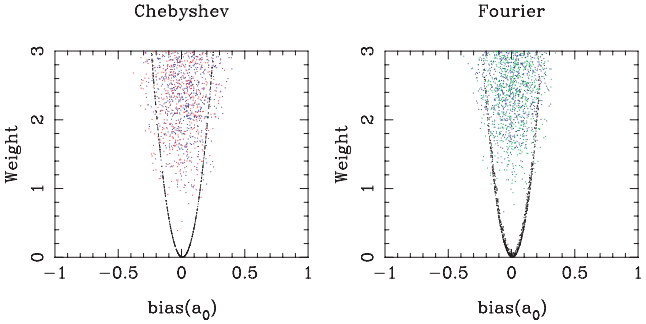

Figure 9. The weight (fit to the systematic data) against the bias in the parameter a_0 for the toy data bounded systematic shown in Fig. 4. We truncate the Chebyshev and Fourier basis sets at $N = 1$ (black dots) $N = 10$ (red, green – light-grey dots) and $N = 50$ (blue, dark grey dots). For each order, we make 500 realizations of the basis set.

reproduced these plots but using various truncated basis sets. Note that the MSE from the bias and marginalization is the same given a parametrization as shown in Appendix A – marginalizing is like functional form filling but with a very restricted class of function.

Fig. 9 shows the weight (fit to data) versus bias using the simple toy model for the Chebyshev and Fourier truncated basis sets for 500 realizations of each truncated set. We truncate the expansion at $N = 1$, 10 and 50. It can be seen that if $N = 1$ is used the space of functions is very restricted, and as the order is increased the space of functions increases. These results are also in resonance with Appendix B. If one were marginalizing, a choice of parametrization (basis and order) would have to be made in which case the MSE conclusion would be dependent on this choice.

4.4 Discussion

We take this opportunity to discuss the difference between marginalizing and functional form filling. Functional form filling is not the same as marginalizing over a very large parameter set on a qualitative level: we are not finding the best-fitting values of the parameters but rather using each parameter combination simply as a prescription that yields a particular bias. As the freedom in the functions increases (more parameters), the functional form-filling approaches a stable regime in the results it gives. Functional form filling yields the probability that the maximum-likelihood value is biased by some amount, whereas marginalization yields a probability that the cosmological parameters take some value jointly with some values of the nuisance parameters.

One could marginalize over a very large number of parameters, but in this case the joint covariance matrix will at some point necessarily become computationally singular as parameters introduced cannot be constrained by the data. One way to consistently include more parameters than data points N is to add a prior such that any extra parameters were constrained $P(A|D) = \int \mathrm{d}B\, P(A, B|D)P(B)$, where $A = N$ and $(A + B) > N$; but this requires adding the prior on $P(B)$ which requires justification.

In the lack of any external prior, the number of parameters that can be used in marginalizing is necessarily truncated at a low order since once the number of free parameters becomes larger than the number of data points (for the data bound) the parameter fitting methodology becomes ill-posed (e.g. Sivia 1996). In contrast, the functional form-filling technique could use an infinite basis set expansion (only computational, and physical, resources prohibit this) since we use the basis set simply as *a prescription for drawing functions* through

the systematic – one could even draw these by hand if you were sure that you could draw a complete set of functions.

One may be concerned that information is being ignored or discarded. Quite the opposite from discarding information present in data, we assign a weight to every possible function with respect to the data, in this sense we throw nothing away – every function has a weight and a bias. In contrast, when marginalizing the functional space assessed is limited by the number of data points and as such a very large class of functions is never considered – if a basis set is truncated, these are usually highly oscillatory functions.

The bias formalism becomes preferable if there is uncertainty over what the functional form is (which is most, if not all of the time).

In Appendix A, we show that for the same basis set and prior functional form filling and marginalization produce the same results in an MSE sense. Hence, in the limit of marginalizing over functions, with suitable priors, the two approaches should produce the same results – in this article, we focus on bias functional form filling.

4.5 Summary

We have presented an algorithm by which any function within a bounded region can be drawn. This is summarized as follows.

(i) Choose a complete orthogonal basis set. We recommend Chebyshev polynomials because of their ease of calculation and computational efficiency (see Appendix B).

(ii) Use equation (21) to calculate the interval $a_n \in [-Q, Q]$ over which the coefficient must be sampled.

(iii) Define the bounded region $B(x)$ within which functions must be drawn.

(iv) Define a scale Δx upon which the functional space must be complete.

(v) Randomly and uniformly sampled from the space of coefficients using a maximum order N and number of realizations such that the functional space is fully filled – the diagnostic tools from Appendix B can be used to gauge the level of completeness.

By defining the hard and data bounds, we have now presented all the tools needed to correctly assess a systematic given some prior knowledge of the magnitude of the effect, either an external data set or some theoretical knowledge. In the hard boundary case, every function is given equal weight and as such a maximum bias should exist. In the data boundary case, a probability can be assigned to each bias.

We emphasize here that this method requires there to be at least *some* information at every data point associated with the signal – either a hard boundary or some systematic data. If there were no constraint, the ranges of biases could become unbounded.

Our proposal is that when measuring some cosmological parameters, these techniques can be used to augment the statistical marginal error contours: some cosmological parameters are measured and about their maximum-likelihood point are drawn some marginalized statistical error contours, and in addition:

(i) if a theory or simulation provides a hard boundary to some systematic, then the maximum bias will define a systematic contour that can be drawn in within which the maximum likelihood could be biased,

(ii) if some data are provided that measures the systematic, then a further set of systematic contours can be drawn which will show the probability that the maximum-likelihood point is biased by any particular amount.

The goal for any experiment is to control systematic effects to such a degree that any systematic contours drawn are smaller than the statistical contours.

We will use the functional form-filling approach in the next section to place requirements on weak lensing systematics. For general conclusions, please skip to Section 6.

5 AN APPLICATION TO COSMIC SHEAR SYSTEMATICS

We will now use the functional form-filling approach to address shape measurement systematics in cosmic shear (due to methods Heymans et al. 2006; Massey et al. 2007; or PSF inaccuracies Hoekstra 2004; Paulin-Henriksson et al. 2008). This section represents an extension of the work of Amara & Refregier (2008) where certain particular functional forms were investigated. Here, we extend the analysis to include all functional behaviour to fully address the impact of the systematic. For a thorough exposition of cosmic shear, we encourage the reader to refer to these extensive and recent reviews and web sites (Bartelmann & Schneider 2001; Wittman 2002; Refregier 2003; Munshi et al. 2008; http://www.gravitationallensing.net). The source code related to the work in this section is released through http://www.icosmo.org, see Appendix F for details.

5.1 Background

Cosmic shear tomography uses both the redshift of a galaxy and the gravitational lensing distortion, shear, to constrain cosmological parameters. The observable in this case is the lensing power spectrum as a function as redshift and scale $C_\ell(z)$. Since we have redshift information, the galaxy population is split into redshift bins where each bin has its own autocorrelation function and the cross-correlations between bins are also to be taken.

Throughout this section, we will use a fiducial cosmology of $\Omega_\mathrm{m} = 0.3$, $\Omega_\mathrm{DE} = 0.7$, $\Omega_\mathrm{B} = 0.0445$, $h = 0.7$, $w_0 = -0.95$, $w_a = 0.0$, $\sigma_8 = 0.9$, $n_\mathrm{s} = 1.0$, where we parametrized the dark energy equation of state using $w(z) = w_0 + w_a(1 - a)$ (Chevallier & Polarski 2001; Linder 2003) and included the spectral index n_s, we consider non-flat models throughout where $\Omega_k = 1 - \Omega_\mathrm{m} - \Omega_\mathrm{DE}$. We assume a weak lensing survey (similar to the DUNE/Euclid proposal; Refregier et al. 2008a) which has an area $= 20\,000$ deg^2, a median redshift of $z_\mathrm{m} = 0.8$ [using the $n(z)$ given in Amara & Refregier 2008] with a surface number density of 40 galaxies arcmin^{-2}. We also assume a photometric redshift error of $\sigma_z(z) = 0.03(1 + z)$ and split the redshift range into 10 tomographic bins.

The observed lensing power spectrum can be written as a sum of signal, systematic and noise terms

$$C_\ell^\mathrm{obs} = C_\ell^\mathrm{lens} + C_\ell^\mathrm{sys} + C_\ell^\mathrm{noise}, \tag{32}$$

so that an estimator of the observed lensing power spectrum can be written by subtracting the shot-noise term C_ℓ^noise

$$\widehat{C_\ell^\mathrm{lens}} = C_\ell^\mathrm{lens} + C_\ell^\mathrm{sys}, \tag{33}$$

where C_ℓ^lens is the underlying true lensing power spectrum, dependant on cosmology, which we want to measure and C_ℓ^sys is some residual systematic. The error on this estimator can be written as

$$\Delta C_\ell = \sqrt{\frac{1}{(2\ell + 1) f_\mathrm{sky}}} \left(C_\ell^\mathrm{lens} + C_\ell^\mathrm{sys} + C_\ell^\mathrm{noise}\right) \tag{34}$$

note that this is the error on the observed signal, not the observed signal itself, so that as the systematic increases the error on the

Table 4. The marginal error on each cosmological parameter for the fiducial weak lensing survey with no residual systematic. Note that no priors have been added on any parameter.

Parameter	Marginal error
$\Omega_{\rm m}$	0.006
Ω_{DE}	0.036
$\Omega_{\rm B}$	0.015
h	0.086
w_0	0.046
w_a	0.152
σ_8	0.009
$n_{\rm s}$	0.019

observed C_ℓ increases. The Fisher matrix and bias are then defined in the usual way (equations 5 and 12) where $\sigma_C = \Delta C_\ell$. Table 4 shows the expected marginal errors on the cosmological parameters using the fiducial survey calculated using the Fisher matrix formalism, note that no prior has been added to these results, they are for lensing alone.

The additive systematic which we consider here is a special kind that has the same shape as the lensing power spectrum but where it is multiplied by some unknown systematic function (sometimes referred to as a multiplicative systematic) A_1 (we use the notation of Amara & Refregier 2008)

$$C_\ell^{{\rm sys},ij} = A_1 C_\ell^{ij}, \tag{35}$$

where ij means the correlation between redshift bins i and j, an autocorrelation is where $i = j$. The particular form of multiplicative bias we consider is that which causes the true shear, as function of angle and redshift $\gamma^{\rm lens}(\theta, z)$, to be incorrectly determined such that the residual systematic shear $\gamma^{\rm sys}(\theta, z)$ is related to the true shear by some function $m(z)$

$$\gamma^{\rm sys}(\theta, z) = m(z)\gamma^{\rm lens}(\theta, z). \tag{36}$$

So that the systematic given in equation (35) can be written $C^{{\rm sys},ij} = [m(z_i) + m(z_j)]C^{ij}{}_\ell$. This expression from Amara & Refregier (2008) actually assigns an $m(z)$ to each redshift slice where each $m(z)$ is the bin-weighted average. A more accurate approach is to include $m(z)$ in the integrand of the lensing kernel ($\xi_{+/-}$ in appendix A of Amara & Refregier 2008). We compared results when the bin-weighted average was used against the correct integral method and found exact agreement, this is because the bins are narrow and the functional variation on subbin-width scales is small.

We note that Huterer et al. (2006) have used Chebyshev polynomials in weak lensing systematic analysis, although they marginalize over a systematic parametrized using Chebyshev polynomials and then investigate the biases introduced if the most likely value of the estimated coefficients were incorrect. Here, we are not measuring the Chebyshev coefficients but rather using this basis set to draw every possible function and determine the bias introduced by the function itself not some misestimation of any particular coefficient. The approach outlined in this article also has a resonance with the work of Bernstein (2008) in which flexible basis sets are used to address systematic quantities, although this is done within the self-calibration (marginalizing) framework, and their general thesis is that of tuning the models that are marginalized over. Bernstein (2008) notes that an approach such as the one outlined in this article, using the formalism of Amara & Refregier (2008), would be desirable in certain situations.

5.2 Functional form filling for $m(z)$

We will now place constraints on the function $m(z)$ such that that the measurement of the cosmological parameters are robust. We first define some boundary (bound function) on $m(z)$ such that any systematic function must lie within the bounded region. We parametrize the hard boundary (Section 4.1) using

$$|m(z)| = m_0(1+z)^\beta, \tag{37}$$

we want to know what values of m_0 and β are sufficient to ensure that the bias on cosmological parameters $b(\theta_i)$ are less than their statistical error $\sigma(\theta_i)$; $|b(\theta_i)/\sigma(\theta_i)| \leq 1$. We stress that this is a parametrization of the *boundary* within which a function must lie, not the function itself.

To fill the bounded area with every functional form, complete down to the scale of $\Delta z = 0.2$, we use Chebyshev polynomials with a maximum order of $N = 35$ and investigate $N_F = 10^4$ realizations of the basis set, using the formalism outlined in Section 4. We do not expect any of the cosmological parameters to introduce features into the lensing power spectrum on scales $\Delta z < 0.2$, so this should be sufficient. Fig. 10 uses the diagnostic measure described in Appendix B to show that on the scale of $\Delta z = 0.2$ every possible functional behaviour has been experienced at every point within the bounded region, for this example we use $m_0 = 1 \times 10^{-3}$ and $\beta = 1.0$.

To begin we will first consider $m(z)$ with $m_0 = 1 \times 10^{-3}$ and $\beta = 1.0$. Using the functional form-filling technique, we have identified which systematic functions cause the largest bias for each cosmological parameter. Table 5 shows the maximum bias to marginal

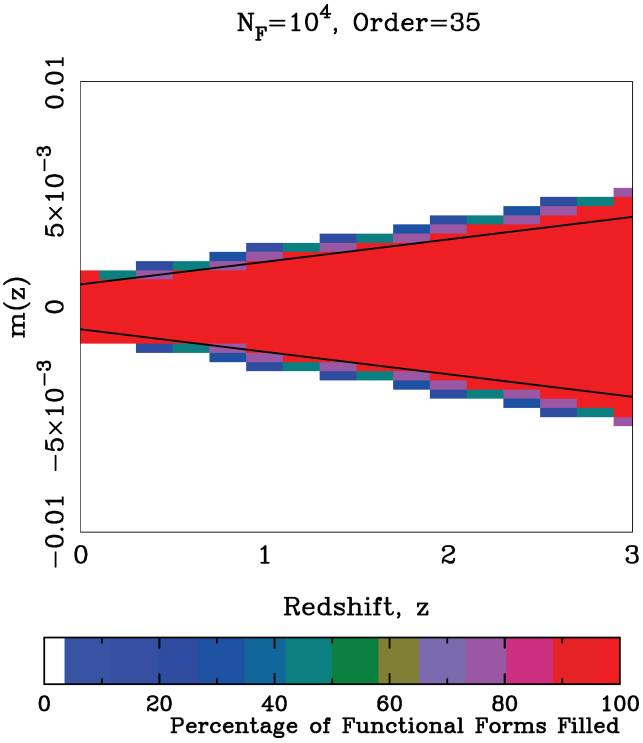

Figure 10. This plot shows the bounded area defined using equation (37) with $m_0 = 1 \times 10^{-3}$ and $\beta = 1.0$, shown by the solid black lines. This area is then pixelated, and the functional behaviour that can occur at each pixel is measured. The colours correspond to the percentage of functional behaviour that has been experienced for each pixel, this is described in detail in Appendix B.

Table 5. The ratio of bias to marginal error for each cosmological parameter for the fiducial weak lensing survey and a multiplicative systematic of the form given in equation (37) with $m_0 = 1 \times 10^{-3}$ and $\beta = 1$. A negative value implies that the bias is negative.

Parameter	Bias/marginal error
$\Omega_{\rm m}$	−0.837
Ω_{DE}	0.813
$\Omega_{\rm B}$	−0.481
h	−0.483
w_0	1.253
w_a	−0.999
σ_8	0.855
$n_{\rm s}$	0.868

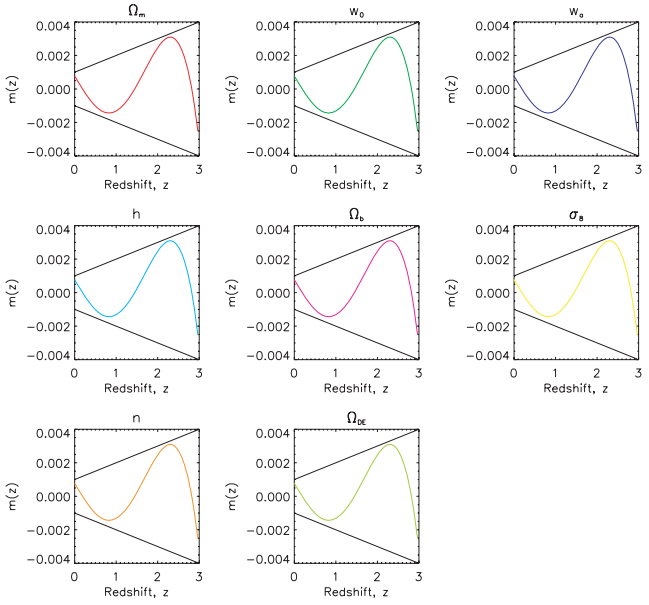

Figure 11. This plot shows the bounded area defined using equation (37) with $m_0 = 1 \times 10^{-3}$ and $\beta = 1.0$, shown by the solid black lines. Plotted within this area are the functions, out of all the possible functions that could be drawn within the bounded region, that cause the largest bias on each cosmological parameter, denoted by the panel title.

error ratio for each cosmological parameter due to this particular $m(z)$.

We have taken into account all degeneracies between parameters in this exercise – in the terminology of equation (12), the inverse Fisher matrix is marginalized over all parameters and the B_j takes into account degeneracies between the cosmology and systematic functions.

Fig. 11 shows the worst functions, that cause the largest bias, for each cosmological parameter. Since there are degeneracies between all parameters, the worst function is practically the same for all parameters.

We find that the ratio of the maximum bias to the marginal error is <1 for most parameters, except $b(w_0)/\sigma(w_0) = 1.25$ which is not acceptable: the bias is larger than the statistical error. These results are in rough agreement with Amara & Refregier (2008) where it was concluded, with a restricted functional parametrization of $m(z)$, and the assumption of a flat Universe that $m_0 = 1 \times 10^{-3}$ and

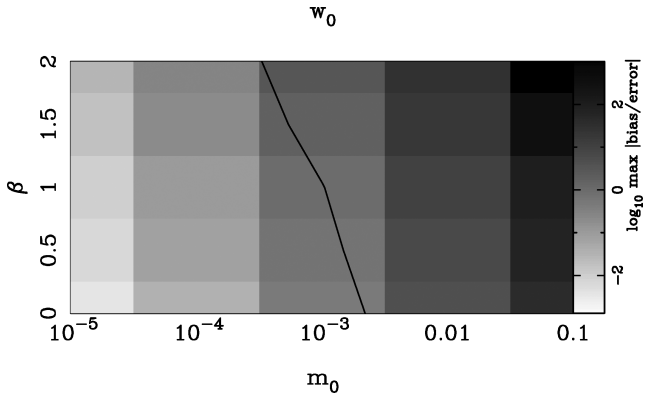

Figure 12. The ratio of maximum bias, found using functional form filling, to marginal error as a function of m_0 and β for w_0. The grey scale represents the bias to error ratio with a key given on the side of each panel. The solid lines show the $b(\theta_i)/\sigma(\theta_i) = 1$ contours for each parameter.

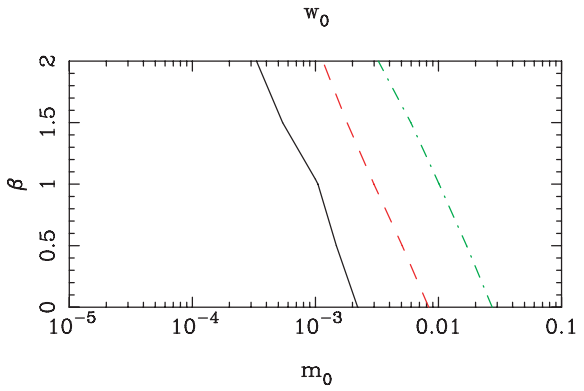

Figure 13. The solid lines show the $|b(w_0)/\sigma(w_0)| = 1.0$ contours in the (m_0, β) parameter space for varying survey area. Black (solid) shows the contour for the fiducial survey with area = 20 000 deg^2, red (light-grey, dashed line) shows the contour for a survey exactly the same as the fiducial survey expect that area = 2000 deg^2 and green (lightest grey, dot-dashed line) for a survey with area = 200 deg^2. For the w_0 constraint to be robust to $m(z)$ systematics, the values of m_0 and β must lie leftwards of the contours, see Fig. 12.

$\beta = 1$ yielded biases that were $b(\theta_i)/\sigma(\theta_i) < 1.0$ but were somewhat on the limit of what is acceptable. Furthermore, it was concluded that functions which have a variation (cross from positive to negative) about $z \gtrsim 1$ have the largest effect, we also find that the functions that cause the largest bias in all the parameters varies in the region of $z \sim 1$. This is because it is at $z \sim 1$ that dark energy begins to dominate and so the parameters w_0 and w_a, and through degeneracies the other parameters, are affected by systematic functions that introduce variation at this redshift.

Fig. 12 shows the ratio of bias to marginal error as a function of m_0 and β for w_0. It can be seen that the redshift scaling β has the expected effect on the maximum systematic bias: as β increases the maximum bias for a given m_0 also increases as the systematic bounded area expands. The solid lines in Fig. 12 show the $b(\theta_i)/\sigma(\theta_i) = 1$ contours. For $m_0 = 1 \times 10^{-3}$, we need a $\beta \lesssim 0.70$ for the bias on w_0 to be acceptable. If the redshift scaling is eliminated $\beta = 0$, then the requirement on the absolute magnitude of $m(z)$ is relaxed to $m_0 \lesssim 2 \times 10^{-3}$.

Fig. 13 shows the affect of survey area on the requirement of m_0 and β. The lines in this figure show the $|b(w_0)/\sigma(w_0)| = 1.0$ contours for varying survey area. We have picked w_0 as an example

since this parameter provides the most stringent constraints on the shape measurement parameters (see Table 5 and Fig. 12). As the survey area increases and the marginal error on w_0 decreases, the requirement on shape measurement accuracy becomes more stringent. We have fitted a simple scaling relation to these contours, so that for statistical errors to be reliable the following relation holds:

$$0.17 \left(\frac{m_0}{1 \times 10^{-3}} \right)^{2.4} \left(\frac{\text{area}}{20\,000} \right)^{1.5} 10^{\beta} \leq 1. \quad (38)$$

The requirements on m_0 and β for the largest survey considered are at the limit of currently available shape measurement techniques that yield on average $m \sim 2 \times 10^{-3}$ at best (Kitching et al. 2008b; Miller et al. 2007). A large redshift variation of $m(z)$ results in large biases (Fig. 11) so a shape measurement method that is unaffected by the magnitude/size of the galaxy population should yield robust cosmological constraints. For example, Kitching et al. (2008b) have shown that the LENSFIT method has a characteristic m that has a small magnitude/size dependence. In this case, $\beta \ll 1.0$, and a more relaxed constraint on $m_0 \sim 2 \times 10^{-3}$–$4 \times 10^{-3}$ is required which is well within reach of these most recent developments in shape measurement. These results are also in agreement with Semboloni et al. (2008) where they find that for a very restrictive class of $m(z)$ functions, of the form $m(z) = az + b$, but a more complex likelihood description, that some parameter combinations of a and b can give rise to biases that are less that the cosmological errors.

For the smaller surveys considered, that are well matched to the currently available or upcoming experiments (e.g. CFHTLS, van Waerbeke et al. 2001; Pan-Starrs, Kaiser et al. 2002), the shape measurement techniques currently available have biases m (Heymans et al. 2006; Massey et al. 2007; Kitching et al. 2008b) that are well within the required level of accuracy. The caveat to these conclusions is that here we have not discussed the size or galaxy-type dependence of any bias and have not considered any calibration offset in the measured shear.

6 CONCLUSION

In this article, we have presented a method that allows one to move beyond the tendency to treat a systematic effect as a statistical one. When a systematic is treated as a statistical signal, extra parameters are introduced to describe the effect, and then these extra nuisance parameters are marginalized over jointly with cosmological parameters. We have shown that even in a very simple toy model such an approach is risky at best. The results being highly dependent on the choice of parametrization, and in the limit of a large number of parameters any statistical signal on cosmological parameters can be completely diluted. One could use marginalization if there exists a compelling physical theory for the systematic, however if the functional form is merely phenomenological or if it contains a truncated expansion then one should use caution. Even in the case that confidence is high with respect to the assumed functional form any residual must be investigated correctly.

As an alternative we advocate treating a systematic signal as such, an unknown contaminant in the data. We address the situation where we have at least some extra information on the systematic, either from some theory or simulation that may provide a hard boundary within which a systematic must lie, or from some external data set. We leave the case of 'entangled systematics' (where there is no extra information and where the systematic depends on the cosmological parameters) to be investigated in Amara et al. (in preparation). Throughout we have introduced each concept using a simple toy model.

Since the systematic is treated as a genuine unknown, we must address every possible functional form that is allowed, by either the hard boundary or the extra systematic data. To do this, we use complete basis sets and randomly sample from the space of coefficients until all functional behaviours have been experienced at every point with the hard boundary, or within a few σ of the data. We have shown that such 'functional form filling' can be achieved by this technique using either Chebyshev, Fourier or top-hat basis sets. By treating each function as a possible systematic, a bias in the maximum-likelihood value is introduced whilst the marginal error stays the same. Throughout we have shown that as long as functional filling is achieved, all conclusions on the magnitude of a systematic effect are independent of the choice of complete basis set – though binning is highly inefficient in terms of computational time, and could be labelled as an unphysical basis set.

For the case of a hard boundary, every function is given an equal probability and as such a maximum bias exists. For the case of extra systematic data, we show that a probability can be assigned to each function, and bias, allowing for the production of robust systematic probability contours.

We have made a first application of hard boundary functional form filling by addressing multiplicative systematics in cosmic shear tomography; we have left an application of the data bound for future work. We address a lensing systematic, that can result from shape measurement or PSF reconstruction inaccuracies, that has the same overall shape as the lensing power spectrum but is multiplied by some extra function. This is commonly represented using a multiplicative function $m(z)$ (Heymans et al. 2006; Massey et al. 2007) where $\gamma^{\rm sys} = m(z)\gamma^{\rm true}$. For a DUNE/Euclid-type survey, we find that in order for the systematic on w_0 to yield a bias smaller than the marginal error the overall magnitude of $m(z)$ should be $m_0 \leq 8 \times 10^{-4}$ for a linear scaling in $(1 + z)$, but as the magnitude of the redshift scaling is relaxed then the requirement on m_0 increases to $m_0 \leq 2 \times 10^{-3}$. The most recent shape measurement methods have $m \sim 2 \times 10^{-3}$ (e.g. using the LENSFIT method Miller et al. 2007; Kitching et al. 2008b) and have a small scaling as a function of magnitude/size. The results shown here then, coupled with some currently available shape measurement techniques, imply that constraints on cosmological parameters from tomographic weak lensing surveys should be robust to shape measurement systematics (with the caveat that PSF calibration and galaxy size dependence of the bias have been neglected here).

The techniques introduced here should have a wide application in cosmological parameter estimation: in any place in which there is some signal with some extra information on a systematic. For example, baryon acoustic oscillations and galaxy bias, cosmic microwave background and foregrounds, galaxy clusters and mass selection, supernovae and light rise times, weak lensing and photometric redshift uncertainties. A sophistication of these techniques could assign different weights/prior probabilities to particular functional forms, that are known a priori to have a large/small effect on cosmological parameter determination; such weights could come from either theoretical or instrumental constraints.

Cosmology is entering into a phase in which the statistical accuracy on parameters will be orders of magnitude smaller than anything achieved thus far. But we must take care of systematics in a rigorous way to be sure that our statistical constraints are valid. There exists the pervading worry that the functional forms used to parametrize systematics are not representative of the true underlying nature of the systematic and that something may have been missed. In such a scenario, one should always add the warning that

'cosmological constraints are subject to the assumption of the systematic form'.

Here, we have presented a way to address systematics in a way that requires no external assumptions, allowing for robust and rigorous statements on systematics to be made.

ACKNOWLEDGMENTS

TDK is supported by the Science and Technology Facilities Council, research grant no. E001114. AA is supported by the Swiss Institute of Technology through a Zwicky Prize Fellowship. FBA is supported by an Early Careers Fellowship from The Leverhulme Foundation. BJ is supported by the Deutsche Telekom Stiftung and by the Bonn-Cologne Graduate School of Physics and Astronomy. We thank Andy Taylor for many detailed discussions on functional form filling. We thank the organizers and participants of the Intrinsic Alignments and Cosmic Shear Workshop at UCL on 2008 March 31–April 4. In particular, Sarah Bridle, Catherine Heymans, Rachel Mandelbaum, Lindsay King, Bjoern Schaefer and Oliver Hahn. We would also like to thank all members of the DUNE/Euclid weak lensing working group. We also thank Eric Linder, Lance Miller, Anais Rassat and a rigorous referee for many insightful discussions.

REFERENCES

Albrecht A. et al., 2006, preprint (arXiv:astro-ph/0609591)
Amara A., Refregier A., 2007, MNRAS, 381, 1018
Amara A., Refregier A., 2008, MNRAS, 391, 228
Abazajian K., Dodelson S., 2003, Phys. Rev. L, 91, 1301
Bartelmann M., Schneider P., 2001, Phys. Rev., 340, 291
Bernstein G., 2008, ApJ, 695, 652
Bridle S., Abdalla F. B., 2007, ApJ, 655, 1
Bridle S., King L., 2007, New J. Phys., 9, 444
Brown M. L., Taylor A. N., Bacon D. J., Gray M. E., Dye S., Meisenheimer K., Wolf C., 2003, MNRAS, 341, 100
Catelan P., Kamionkowski M., Blandford R., 2001, MNRAS, 320, 7
Chevallier M., Polarski D., 2001, International J. Modern Phys. D, 10, 213
Cooray A., 1999, A&A, 348, 31
Crittenden G., Natarajan P., Pen U.-L., Theuns T., 2001, ApJ, 559, 552
Fisher R., 1935, J. R. Stat. Soc., 98, 35
Hannestad S., Wong Y., 2007, J. Cosmol. Astropart. Phys., 07, 004
Heavens A. F., Refregier A., Heymans C., 2000, MNRAS, 319, 649
Heavens A. F., Kitching T. D., Verde L., 2007, MNRAS, 380, 1029
Heymans C., Heavens A. F., 2003, MNRAS, 339, 711
Heymans C. et al., 2006, MNRAS, 368, 1323
Hirata C., Seljak U., 2004, Phys. Rev. D, 70, 3526
Hoekstra H., 2004, MNRAS, 347, 1337
Huterer D., Takada M., 2005, Astroparticle Phys., 23, 369
Huterer D., Masahiro T., Bernstein G., Jain B., 2006, MNRAS, 366, 101
Joachimi B., Schneider P., 2008, A&A, 488, 829
Jungman G., Kamionkowski M., Kosowsky A., Spergel D., 1996, Phys. Rev. D, 54, 1332
Kaiser N. et al., 2002, Proc. SPIE, Vol. 4836, p. 154
Kim A., Linder E., Miquel R., Mostek N., 2004, MNRAS, 347, 909
King L. J., Schneider P., 2003, A&A, 398, 23
Kitching T. D., Taylor A. N., Heavens A. F., 2008a, MNRAS, 389, 173
Kitching T. D., Miller L., Heymans C., Heavens A. F., Van Waerbeke L., 2008b, MNRAS, 390, 149
Kitching T. D., Heavens A. F., Verde L., Serra P., Melchiorri A., 2008c, Phys. Rev. D, 77, 103008
Kitching T. D., Amara A., Rassat R., Refregier A., 2008d, A&A, submitted
Kunz M., Sapone D., 2007, Phys. Rev. Lett. 98, l21301
Linder E., 2003, Phys. Rev. Lett., 90, 091301
Massey R. et al., 2007, MNRAS, 376, 13
Miller L., Kitching T. D., Heymans C., Heavens A. F., Van Waerbeke L., 2007, MNRAS, 382, 315
Munshi D., Valageas P., van Waerbeke L., Heavens A., 2008, Phys. Rep., 462, 67
Paulin-Henriksson S., Amara A., Voigt L., Refregier A., Bridle S. L., 2008, A&A, 484, 67
Peacock J., Schneider P., 2006, Messenger, 125, 48
Pedersen K., Dahle H., 2007, ApJ, 667, 26
Refregier A., 2003, ARA&A, 41, 645
Refregier A. et al., 2008a, Proc. SPIE, 23–28 June
Refregier A., Amara A., Rassat R., Kitching T., 2008b, A&A, submitted
Semboloni E., Tereno I., Heymans C., van Waerbeke L., 2008, MNRAS, 397, 608
Seo H., Eisenstein D., 2003, ApJ, 598, 720
Sivia D. A., 1996, Oxford Univ. Press, Clarendon Press
Taylor A. N., Kitching T. D., Bacon D. J., Heavens A. F., 2007, MNRAS, 374, 1377
Tegmark M., Taylor A., Heavens A., 1997, ApJ, 440, 22
Wittman D., 2002, Lect. Notes Phys., 608, 55
van Waerbeke L. et al., 2001, A&A, 347, 757

APPENDIX A: MARGINALIZATION VERSUS BIAS

Here, we will show how marginalization is mathematically different to the bias formalism used in the main article.

When marginalizing the log-likelihood of some cosmological parameters $\boldsymbol{\theta}$ can be written for a signal C some theory T and a systematic S as

$$2\mathcal{L}(\boldsymbol{\theta}) = \sum_x \sigma_C^{-2}(C - T - S)^2. \tag{A1}$$

When marginalizing over the systematic, the effect is parametrized by some extra parameters $\boldsymbol{a}$. If extra data D is provided on the systematic then this adds a prior such that the total log-likelihood can be written as

$$2\mathcal{L}(\boldsymbol{\theta}, \boldsymbol{a}) = \sum_x \sigma_C^{-2}(C - T - S)^2 + \sum_x \sigma_D^{-2}(D - S)^2. \tag{A2}$$

The Fisher matrix for this is created by taking the derivatives of the log-likelihood with respect to cosmological parameters $\boldsymbol{\theta}$ and systematic parameters $\boldsymbol{a}$ so that the first and second terms in equation (A2) give the following Fisher matrices:

$$\begin{aligned} F^{\Phi\Phi} &= \begin{pmatrix} F^{\theta\theta} & F^{\theta a} \\ F^{a\theta} & F^{aa} \end{pmatrix}_C + \begin{pmatrix} 0 & 0 \\ 0 & F^{aa} \end{pmatrix}_D \\ &= \begin{pmatrix} F^{\theta\theta} & F^{\theta a} \\ F^{a\theta} & F_C^{aa} + F_D^{aa} \end{pmatrix}. \end{aligned} \tag{A3}$$

The marginal error on the cosmological parameters is found by inverting equation (A3). The inverse of the upper-left segment of the Fisher matrix in equation (A3) can be found by using the Schur complement of the block matrix and then expanding this using the Woodbury matrix identity which gives

$$\begin{aligned} \left(F^{\Phi\Phi}_{\text{upper-left}}\right)^{-1} &= \text{MSE}_{\text{marg}} \\ &= A^{-1} + A^{-1}B(E - B^T A^{-1} B)^{-1} B^T A^{-1}, \end{aligned} \tag{A4}$$

where $A = F^{\theta\theta}$, $B = F^{\theta a}$ and $E = F_C^{aa} + F_D^{aa}$. The marginal error in the case of no systematic (A^{-1}) has been increased by an extra factor that depends on the degeneracies between the systematic parameters and the cosmological ones (B) and on the information available on the systematic parameters themselves (E). This is also equal to the MSE of the cosmological parameters in this case, since no bias is introduced.

For the bias functional form-filling technique, the log-likelihood of the cosmological parameters can again be written as

$$2\mathcal{L}(\boldsymbol{\theta}) = \sum_x \sigma_C^{-2}(C - T - S)^2. \tag{A5}$$

In the data bound case, we can assign a weight to each systematic *function S* (not extra parameters)

$$2\mathcal{L}(S) = \sum_x \sigma_D^{-2}(D - S)^2, \tag{A6}$$

so that a very similar expression to equation (A2) can be written for the joint log-likelihood of the cosmological parameters and the systematic

$$2\mathcal{L}(\boldsymbol{\theta}, S) = \sum_x \sigma_C^{-2}(C - T - S)^2 + \sum_x \sigma_D^{-2}(D - S)^2. \tag{A7}$$

We have not necessarily parametrized S with any parameters we wish to measure, S can simply be a function that has been arbitrarily drawn through the systematic data. However, if the systematic is parametrized (as we do in the functional form-filling approach using complete basis sets) then the signal data C are not used to determine the values of the extra parameters – the number of degrees of freedom in the fit has been reduced with respect to the marginalizing case. The systematic data D (or a hard boundary) is used to determine the probability of the systematic. Hence, the Fisher matrix can be written, in this case, like

$$\begin{aligned} F^{\boldsymbol{\Phi\Phi}} &= \begin{pmatrix} F^{\boldsymbol{\theta\theta}} & 0 \\ 0 & 0 \end{pmatrix}_C + \begin{pmatrix} 0 & 0 \\ 0 & F^{\boldsymbol{aa}} \end{pmatrix}_D \\ &= \begin{pmatrix} F^{\boldsymbol{\theta\theta}} & 0 \\ 0 & F_D^{\boldsymbol{aa}} \end{pmatrix}. \end{aligned} \tag{A8}$$

The inverse of the upper-left segment is now simply $(F^{\boldsymbol{\theta\theta}})^{-1} = A^{-1}$. Using the result from Appendix D (for the hard boundary case), a bias is introduced with a maximum value of

$$\max|b_i| = (\text{constant})(A^{-1})_{ij}\left(\sum \sigma_C^{-2}\frac{\partial C}{\partial \theta_j}\right)^2 = (\text{const})(A^{-1})_{ij}F_j^2. \tag{A9}$$

We have again condensed the notation so that $F_j = \sum \sigma_C^{-2}\frac{\partial C}{\partial \theta_j}$. Note that $F \neq B \neq E$. Hence, the total MSE on cosmological parameters for the bias case comes from the unaffected marginal error of the cosmological parameter and the bias

$$\text{MSE}_{\text{bias}} = A^{-1} + \text{bias}^2 = A^{-1} + (\text{constant})^2(A^{-1})^2F^4. \tag{A10}$$

A similar expression can be written for the data-bound case (see Appendix D, equation D13). We have compressed the subscript notation from equation (A9) in (A10).

These equations show how marginalization and the bias formalism relate in a general sense, and that they are mathematically different objects i.e. when finding the maximum bias using the functional form-filling approach the MSE between marginalization and functional form filling *can* be different. This difference arises because the space of functions probed by marginalization is restricted. In the next section, we will show that if the functional space assessed is the same then the MSE should be equal.

A1 Information content

If the parametrization, and number of (truncated) parameters, is the same then the MSE resulting from the bias or marginalizing is the same. We show this here using a simple illustrative example.

We approximate the nuisance correlation C^{sys} as a first-order expansion of a set of parameters

$$C^{\text{sys}}(\boldsymbol{a}) = C_0^{\text{sys}} + \boldsymbol{a}\dot{\nabla}_a C_0^{\text{sys}}. \tag{A11}$$

This can be though of as a restricted set of functions or a special case of C^{sys}. The nuisance parameters $\boldsymbol{a}$ will be correlated with the cosmological parameters $\boldsymbol{\theta}$ and we can form the extended vector and Fisher matrix as shown in equation (A3); as in equation (A4), we can write the marginalized covariance matrix of $\boldsymbol{\theta}$ like

$$\begin{aligned} \langle \boldsymbol{\theta\theta}^t \rangle_{\text{c}} &= [F_{\Phi\Phi}]^{-1}_{\theta\theta} \\ &= F_{\theta\theta}^{-1} + F_{\theta\theta}^{-1}F_{\theta a}(F_{aa} - F_{\theta a}^t F_{\theta\theta}^{-1}F_{\theta a})^{-1}F_{\theta a}F_{\theta\theta}^{-1}, \end{aligned} \tag{A12}$$

and there is no bias of the measured parameters. The subscript 'c' on the covariance indicates that we are including the covariance between $\boldsymbol{\theta}$ and $\boldsymbol{a}$.

If instead we do not account for the covariance between $\boldsymbol{\theta}$ and $\boldsymbol{a}$ in the data, the measured error in the parameters is

$$\langle \boldsymbol{\theta\theta}^t \rangle = [F_{\theta\theta}]^{-1}, \tag{A13}$$

but we have induced a bias in the measurement of $\boldsymbol{\theta}$,

$$\Delta\boldsymbol{\theta} = -F_{\theta\theta}^{-1}\sum \sigma_D^{-2}\frac{\partial C^{\text{signal}}}{\partial \theta}C^{\text{sys}}(\boldsymbol{a}), \tag{A14}$$

where σ_D^2 is the variance of the data. Using our linear expansion of $C^{\text{sys}}(\boldsymbol{a})$, we find

$$\Delta\boldsymbol{\theta} = -F_{\theta\theta}^{-1}F_{\theta a}\boldsymbol{a}. \tag{A15}$$

From this, can see the bias effect explicitly comes through the correlation of the nuisance parameters with the cosmological parameters, via $F_{\theta a}$.

We can simplify things further by considering a single parameter θ and a single nuisance parameter a. The conditional error on the parameter can be simplified to

$$\langle \theta\theta \rangle_{\text{c}} = \langle \theta\theta \rangle(1 - r^2)^{-1}, \tag{A16}$$

where we have introduced the correlation coefficient defined as

$$r^2 = F_{\theta\theta}^{-1}F_{\theta a}^2F_{aa}^{-1}. \tag{A17}$$

We can see this by looking at the inverse of the 2×2 matrix $F_{\Phi\Phi}$,

$$F_{\Phi\Phi}^{-1} = \frac{1}{F_{\theta\theta}F_{aa} - F_{\theta a}^2}\begin{pmatrix} F_{aa} & -F_{\theta a} \\ -F_{a\theta} & F_{\theta\theta}F_{aa} \end{pmatrix}. \tag{A18}$$

The marginalized error on θ is

$$\langle \theta\theta \rangle_{\text{c}} = \frac{F_{aa}}{F_{\theta\theta}F_{aa} - F_{\theta a}^2} = \langle \theta\theta \rangle(1 - r^2)^{-1}. \tag{A19}$$

Similarly, the marginalized error on a is given by

$$\langle aa \rangle_{\text{c}} = \langle aa \rangle(1 - r^2)^{-1}. \tag{A20}$$

Note that the marginalized errors on θ and a go to infinity when the correlation coefficient is unity, $r = 1$. This is because θ and a are completely degenerate.

From the definition of the correlation coefficient, we can write the covariance between θ and a as

$$\langle \theta a \rangle_{\text{c}}^2 = \langle \theta\theta \rangle_{\text{c}}\langle aa \rangle_{\text{c}}r^2, \tag{A21}$$

which agrees with the definition of r given in equation (A17).

Note that the results for $\langle \theta\theta \rangle_{\text{c}}$, $\langle aa \rangle_{\text{c}}$ and $\langle \theta a \rangle_{\text{c}}^2$ are not just the errors and covariance when we marginalize. They are also the errors and covariances when the parameter θ is correlated with a. The only way to get back the uncorrelated errors is if θ and a are uncorrelated, so $r = 0$, or if we know a from some other measurement, in which

case they effectively decorrelate. Even if we assume some value, or range of values, for a, there is still a correlation between possible values of a and θ.

Now, consider the bias on θ, $\Delta\theta$, when we ignore the nuisance effect (or assume some fixed form) . In our simple model, the bias can be written as

$$\Delta\theta = \frac{\langle\theta\theta\rangle^{1/2}}{\langle aa\rangle^{1/2}}\, ar = \frac{\langle\theta\theta\rangle_{\rm c}^{1/2}}{\langle aa\rangle_{\rm c}^{1/2}}\, ar. \tag{A22}$$

Now, the error on the bias, including all the correlations between parameters, is given by

$$\langle\Delta\theta\Delta\theta\rangle_{\rm c} = \left(\frac{\langle\theta\theta\rangle_{\rm c}}{\langle aa\rangle_{\rm c}}\right)\langle aa\rangle_{\rm c} r^2 = \langle\theta\theta\rangle_{\rm c} r^2 = \langle\theta\theta\rangle\frac{r^2}{1-r^2}. \tag{A23}$$

One might have mistakenly thought that the covariance between θ and a was

$$\langle\Delta\theta\Delta\theta\rangle_{\rm c} = \left(\frac{\langle\theta\theta\rangle}{\langle aa\rangle}\right)\langle aa\rangle r^2 = \langle\theta\theta\rangle r^2, \tag{A24}$$

but in doing so we have ignored the real correlation between θ and a that exists. In the case of fully correlated parameters, when $r = 1$, the error on $\Delta\theta$ is only the uncorrelated error on θ, whereas the real uncertainty is infinite.

Finally, the correlation between the bias and the cosmological parameter is

$$\langle\theta\Delta\theta\rangle_{\rm c} = \frac{\langle\theta\theta\rangle_{\rm c}^{1/2}}{\langle aa\rangle_{\rm c}^{1/2}}\, r\langle\theta a\rangle_{\rm c} = \frac{\langle\theta\theta\rangle_{\rm c}^{1/2}}{\langle aa\rangle_{\rm c}^{1/2}}\, r\langle\theta\theta\rangle_{\rm c}^{1/2}\langle aa\rangle_{\rm c}^{1/2} r = \langle\theta\theta\rangle_{\rm c} r^2. \tag{A25}$$

Now, we want to compare the effect of the bias with marginalization on the error of θ. In the case of marginalization, this is given by the correlated covariance

$$\langle\theta\theta\rangle_{\rm c} = \langle\theta\theta\rangle(1-r^2)^{-1}. \tag{A26}$$

In the case of bias, we have to add the uncorrelated error, $\langle\theta\theta\rangle$, with the error in the bias value, $\langle\Delta\theta\Delta\theta\rangle_{\rm c}$, which does include the correlation between cosmological and nuisance parameters, to form the MSE,

$$\begin{aligned}\mathrm{MSE} &= \langle\theta\theta\rangle + \langle\Delta\theta\Delta\theta\rangle_{\rm c}\\ &= \langle\theta\theta\rangle + \langle\theta\theta\rangle_{\rm c} r^2 = \langle\theta\theta\rangle + \langle\theta\theta\rangle\frac{r^2}{(1-r^2)}\\ &= \langle\theta\theta\rangle(1-r^2)^{-1}\\ &= \langle\theta\theta\rangle_{\rm c}.\end{aligned} \tag{A27}$$

Hence, the MSE is the same as the marginalized error in this simple case, and there is no loss or gain of information. Our result here is for a two-parameter case, but is easily extended to multiple parameters.

It is worth thinking about the assumptions that lead to this result. For instance, we have assumed in our analysis that the nuisance bias is *completely specified* by the parameter α.

This shows that if one fully understands the nuisance effect there is no difference between marginalization and form filling. Given marginalization can be done quickly, and in some cases analytically, we would advocate marginalization in this case.

However, if the form of the nuisance function is not known, or is wrong, marginalization will tend to underestimate the true systematic error because of the limited functional space explored by the set of functions assessed by the truncated basis set.

Given that in general the number of parameters that can be marginalized over is limited by the number of data points if the systematic parametrization is unknown then the marginalizing will necessarily not be able to assess the impact of some functions.

A2 Constraining nuisance effects with external data

The effect of additional, external data to constrain the nuisance effects will add an extra Fisher matrix to F_{aa},

$$F_{aa} \rightarrow F'_{aa} = F_{aa} + F^{\rm ex}_{aa}. \tag{A28}$$

If we define a new parameter

$$\beta = [F_{aa}]^{-1} F^{\rm ex}_{aa} = \frac{\langle aa\rangle}{\langle aa\rangle^{ex}} \tag{A29}$$

as the ratio of the conditional error on a from the original data set to the expected measured accuracy on a from the external data. If the error on a from the external data is small, we can expect β to be large, while of the external error is large β will be small. This results in the correlation coefficient becoming

$$r'^2 = \frac{r^2}{1+\beta}. \tag{A30}$$

When the error on the nuisance parameters is highly constrained by the new data set, $\beta \gg 1$ and the correlation coefficient decreases. The effect of new data in the nuisance functions is to decorrelate the nuisance parameter from the data. Propagating this through, we find

$$\langle aa\rangle'_{\rm c} = \langle aa\rangle\left(\frac{1}{1-r^2+\beta}\right), \tag{A31}$$

so that the improved accuracy from the external data set feeds through. The marginalized error on the cosmological parameter is now

$$\langle\theta\theta\rangle'_{\rm c} = \langle\theta\theta\rangle\left(\frac{1+\beta}{1-r^2+\beta}\right). \tag{A32}$$

The error on the bias is now

$$\langle\Delta\theta\Delta\theta\rangle = \langle\theta\theta\rangle'_{\rm c} r'^2 = \frac{\langle\theta\theta\rangle r^2}{(1-r^2+\beta)}. \tag{A33}$$

Finally, the MSE is

$$\begin{aligned}\mathrm{MSE}' &= \langle\theta\theta\rangle' + \langle\Delta\theta\Delta\theta\rangle'_{\rm c}\\ &= \langle\theta\theta\rangle + \frac{\langle\theta\theta\rangle r^2}{(1-r^2+\beta)}\\ &= \langle\theta\theta\rangle\left(\frac{1+\beta}{1-r^2+\beta}\right).\end{aligned} \tag{A34}$$

Hence, adding an external data set to constrain a does not change the conclusions that, if the systematic effect can be modelled by a known parameterization, the MSE is the same as the marginalized error on θ.

A3 Summary

We summarize this Appendix by stating the its main conclusions

(i) *If* the functional form of the systematic is known then the degradation in the MSE as a result of marginalizing or functional form filling (bias) is the same.

(ii) If the functional form of the systematic is unknown then the MSE from marginalizing will tend to underestimate the true systematic error and is in general not equal to the MSE from functional form filling.

(iii) Given that the marginalizing necessarily truncates the basis set there are always some functions that marginalizing cannot assess.

APPENDIX B: TESTING FUNCTIONAL FILLING

In this Appendix, we will present a numerical analysis that will show that if the order and the number of function evaluations is sufficient then a bounded area can be exhaustively filled with all possible functional forms complete to some scale. We want a non-parametric minimum-assumption approach for determining whether we have fully sampled the allowed function space.

We can pick a certain scale upon which we can investigate whether all possible functional forms are evaluated. Having chosen a scale a bounded area can now be pixelated at that scale. In Fig. B1, we consider a particular pixel and its neighbouring pixels. There are 22 non-degenerate ways in which a function can pass through the pixel in question and two surrounding pixels (entering via one pixel and exiting via another) for example (enter 1, exit 2), (enter 1, exit 3), (enter 1, exit 4), ..., (enter 8, exit 6). We call each combination of entrance and exit a 'functional dependency' or a 'functional behaviour'. We exclude functions that are multiple-valued for example (enter 8, exit 7) which would require multiple values of $y(x)$ for a given x.

Some combinations are more likely than others, for example consider a box centred on (0, 0). The function $y = x$ will enter through 1 and exit via 5, corner functions of this type are unlikely but not impossible, a more robust and fair measure may concatenate boxes 1 and 2 (and 3 and 4) for example.

We now look at *each* and *every* pixel within the bounded region and for each function drawn perform a check of which entrant and exit functional dependencies are explored – checking off each functional dependency as it is sampled. We then assign for each pixel the percentage of functional dependencies that have been experienced as a result of having drawn the full set of functions. We perform this test for the hard boundary toy model presented in Section 3.3 for each of the basis sets considered in Section 4, Chebyshev, Fourier and top-hat functions. We increase the maximum order N in the expansion in equation (22) and the number of random realizations N_F of the coefficient space $\{a_0, \ldots, a_N\}$ (and $\{b_0, \ldots, b_N\}$ for the Fourier basis set).

Figs B2–B4 show the toy model hard boundary that has been pixelated on the scale of $\Delta x = 0.5$. It can be seen that within the bounded area every pixel does experience all functional behaviour if the order and number of functions drawn is sufficiently large. As expected when the functional order increases, and as the number of function evaluations increases, the number of pixels that experience

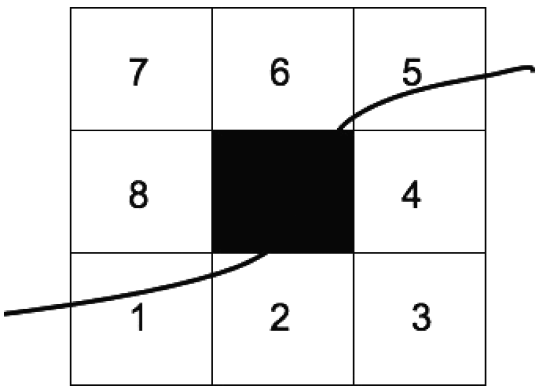

Figure B1. For each pixel defined within a bounded region, we label the neighbouring pixels. The function shown would assign the functional dependency (enter 2, exit 6) to the central pixel.

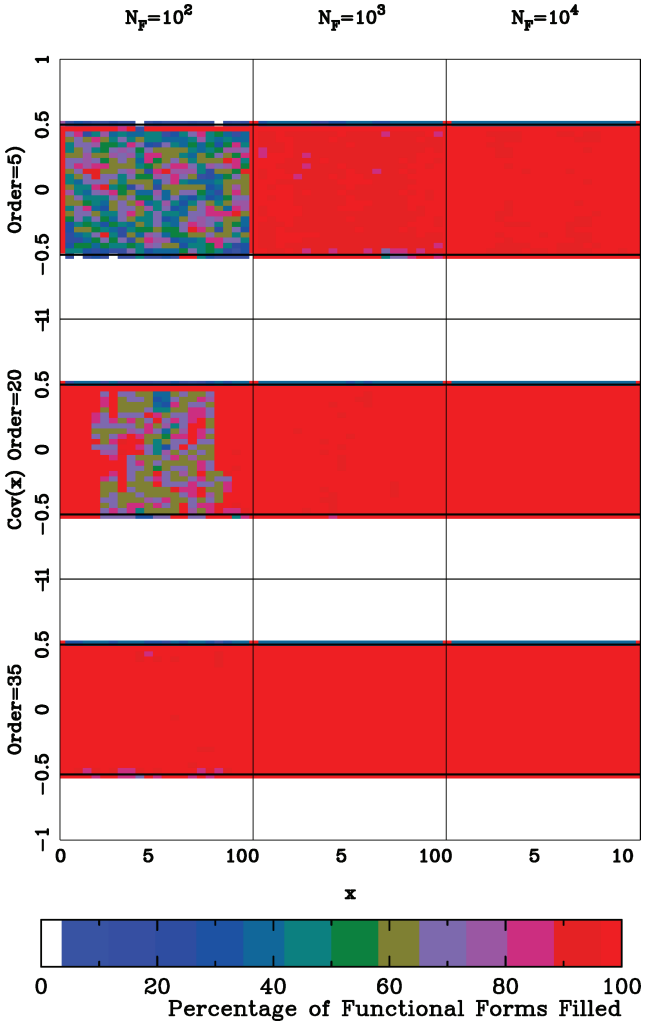

Figure B2. For the Chebyshev basis set. For each pixel defined within the simple bounded region we sum up all functional dependencies experienced from the full set of functions evaluated.

all functional dependencies increases. We find that a maximum order of $N \gtrsim 35$ with $N_F \gtrsim 10^4$ realizations is sufficient for each point in the bounded area to experience every functional form for this simple example.

For the top-hat basis set (binning), we find that the maximum order (number of bins) needs to be much larger than for either Chebyshev or Fourier basis sets. This can be understood since if the bin width (order) is larger than the resolution of the pixels then it is impossible for any given pixel to experience particular functional dependencies (such as [enter 1, exit 2]). So, even though top-hat functions can be used for functional form filling there is some computational expense in this choice.

Fig. B5 shows some diagnostic plots representing the completeness of the functional space sampled. We show the per cent of pixels that have 100 per cent of the possible functional behaviours sampled, and the percentage of functional behaviours sampled by the average pixel. In the top panels, we vary the scale that is investigated, and it can be seen that for the Chebyshev and Fourier basis sets ∼100 per cent of pixels have experienced every functional behaviour down to a scale of $\Delta x \approx 0.5$. The top-hat basis set performs much worse with a mean filling of ∼10 per cent, and only ∼50 per cent of all pixels experiencing every possible

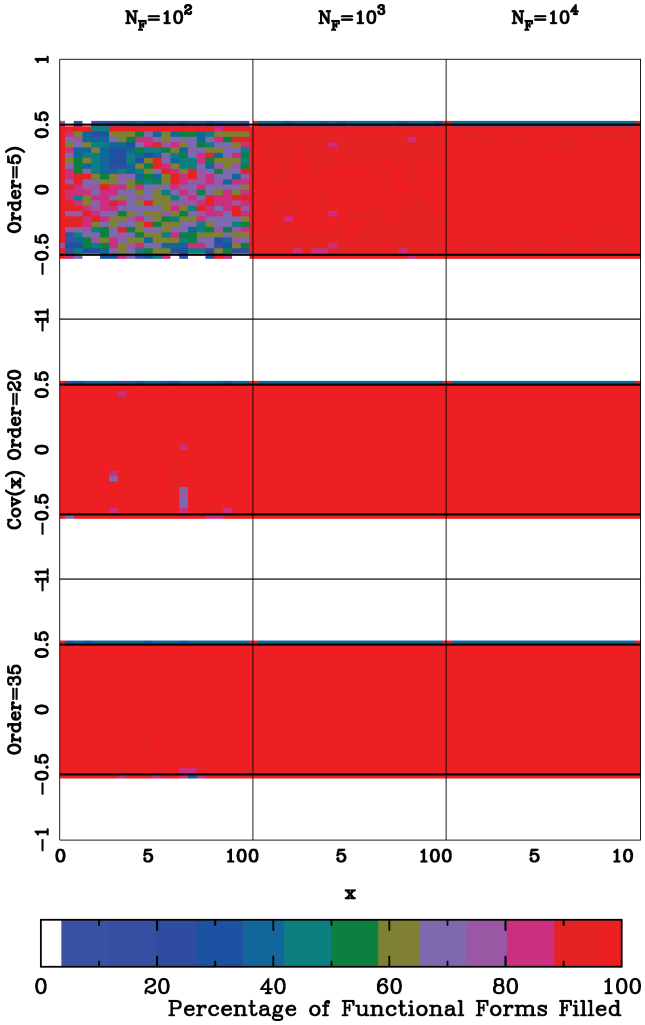

Figure B3. For the Fourier basis set. For each pixel defined within the simple bounded region, we sum up all functional dependencies experienced from the full set of functions evaluated.

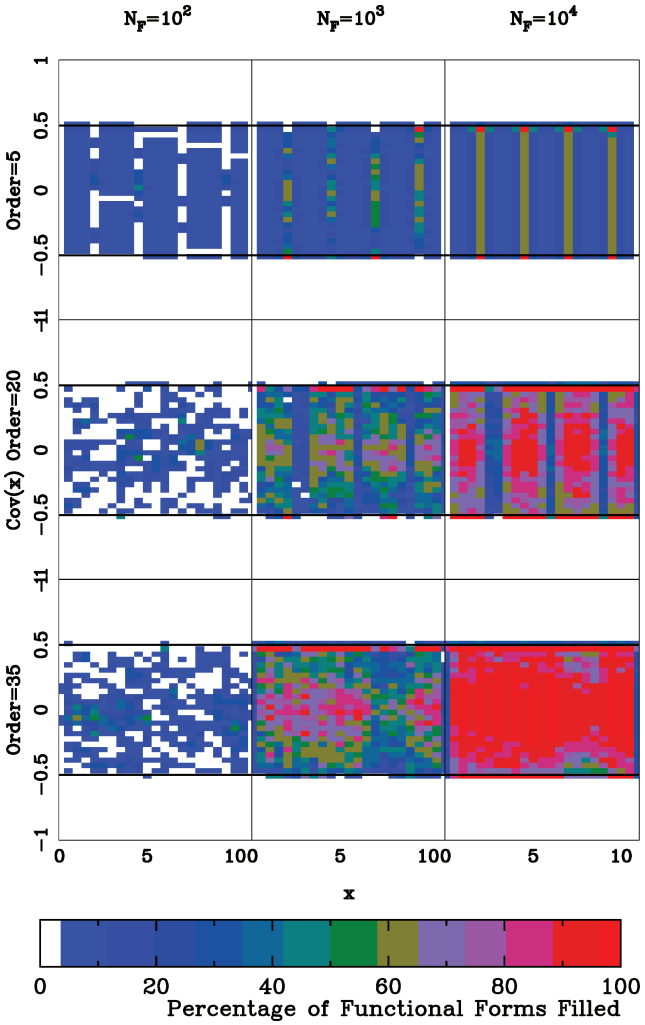

Figure B4. For the top-hat basis set. For each pixel defined within the simple bounded region, we sum up all functional dependencies experienced from the full set of functions evaluated. For the top-hat basis, order corresponds to 'number of bins'.

behaviour. The general trend is that as the scale drops below the average oscillation length of the most highly varying functions the percentage of 'good' pixels (experiencing all functional behaviour) sharply declines. The top-hat basis set fails at $\Delta x \sim 0.3$ since, with $N = 35$ this is approximately the 'bin width' of the functions. In a cosmological application, one would ensure that the form filling was complete down to the scale upon which a particular parameter affects the signal.

In the middle panels of Fig. B5, we vary the maximum order of the basis set expansion whilst keeping both the scale and the number of random realizations fixed. It can again be seen that for a maximum order $\gtrsim$35 the Chebyshev and Fourier basis sets achieve 100 per cent functional filling. Again, the top-hat basis set (binning) fails to achieve any complete functional filling, and only begins to fill in some pixels when the number of bins becomes more than the number of pixels.

The lower panel of Fig. B5 shows how the filling efficiency varies with the number of random realizations of the basis set. For the simple example given the Chebyshev and Fourier basis sets completely fill the bounded area down to the scale of $\Delta x = 0.5$ in $\sim 10^3$ realizations whereas the top-hat basis set requires many orders of magnitude more realizations.

One could imagine further metrics that could be used to gauge the completeness of the functional space that has been sampled; in this first exposition of the methodology, we have shown a simple way to gauge this effect.

One concern is that this metric may favour the top-hat basis since we are using a pixelated measure of scale. However, we find that even with this advantage the top-hat basis set achieves complete filling only at the expense of a prohibitive amount of computational time compared to the Chebyshev and Fourier basis sets, as the order and the number of realizations would need to be much larger to compensate for the pathological choice of basis functions.

We note that a step-function (e.g. function f over the interval $x \in [0, 1]$which is equal to $+1$ for $0 < x < 0.5$ and -1 for $0.5 < x < 1$) may be better approximated by a low-order top-hat function and may take a very high order Chebyshev or Fourier expansion. The feature highlighted here – a step function – has a feature (the step) which has a very small scale variation. In fact, the scale of a step is actually zero. The issue of whether functional form filling is complete down to some scale is shown in Fig. B5, and as the maximum order is increased and more highly oscillatory functions are included the minimum complete scale will decrease. This example highlights

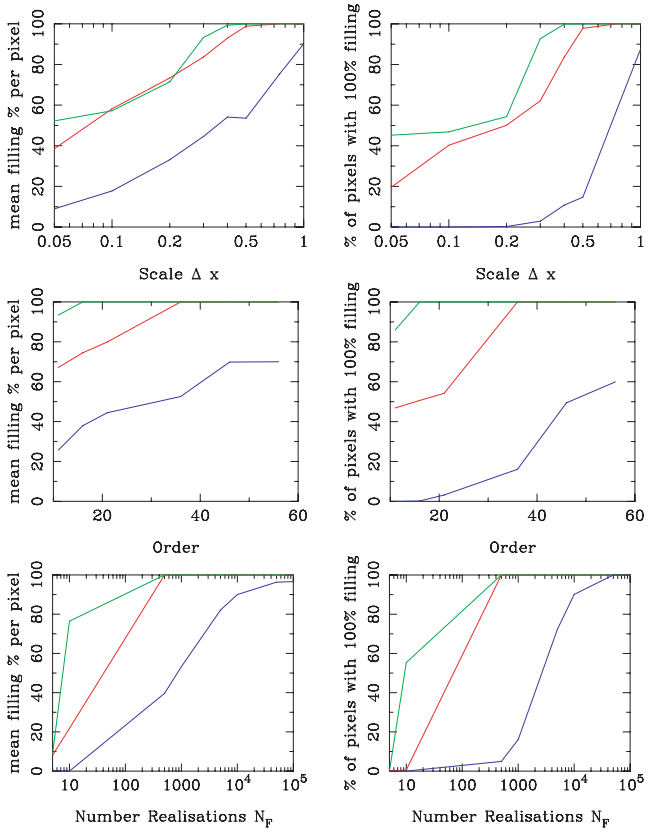

Figure B5. The right-hand panels show the percentage of pixels in the bounded area that have experienced every type of functional behaviour (100 per cent filling). The left-hand hand panels show the percentage of all functional behaviours experienced per pixel on average. The upper panels show these diagnostic measures of functional form filling as a function of scale, with the order and number of realizations fixed at $N = 35$ and $N_F = 10^3$, respectively. The middle panels as a function of maximum order, with the scale and number of realizations fixed at $\Delta x = 0.5$ and $N_F = 10^3$, respectively, and the lower panels as a function of number of random realizations, with the scale and order fixed at $\Delta x = 0.5$ and $N = 35$ respectively. In all panels, blue (darkest grey, lower lines) is for the top-hat (binning) basis set, red (lighter grey) for the Chebyshev basis set and green (lightest grey) for the Fourier basis set.

that fact that the top-hat basis set can probe these very small scales to some degree whilst missing larger scale features, this can be seen in Fig. B4.

For all the calculations in Section 4, we pessimistically use a maximum order of $N = 35$ and use $N_F = 10^4$ realizations for all basis sets.

APPENDIX C: COMPUTATIONAL TIME

One may be concerned at the amount of computational time that the functional form filling we are advocating may take. This is a valid concern since many realizations of the systematic data could be required and one must reperform the cosmological parameter fitting for each and every possible function in order to evaluate the potential bias.

If, for a simple grid search in parameter space, the time taken to analyse a single point in parameter space is τ then for N cosmological parameters the total time-scales as $T \propto A^N \tau$ where A is the number of evaluations per parameter. Even for one parameter $A \gg 1$ to correctly map out a likelihood surface. If one marginalizes over M extra systematic parameters then the total time must increase to $T_{\rm marg} \propto A^{(N+M)}\ \tau$. For the functional form-filling case, the total time taken for the calculation is simply the number of different function evaluations F multiplied by the number of data realizations D and the time to estimate the cosmological parameters is $T_{\rm fff} \propto FDA^N\tau$. The ratio in the computation time can now be written as $T_{\rm marg}/T_{\rm fff} \approx A^M/FD$.

Let us pessimistically assume that approximately $F = 10^4$ function evaluations are needed and $D = 10^3$ data realizations, and conservatively assume that $M = 10$ extra systematic parameters are required to ensure a systematic effect is correctly determined. For $A \gtrsim 100$, we find $T_{\rm marg} \gtrsim 10^9 T_{\rm fff}$. So, on the contrary to such a technique being computationally expensive, treating systematics in such a fashion may in fact be much more efficient than marginalizing over many nuisance parameters using a traditional grid search.

For some Monte Carlo parameter searches, the computational time can be reduced to $T = NA\tau$. In this case, we find that $T_{\rm marg}/T_{\rm fff} \approx M/NFD + 1/FD$. The computation time is now longer for functional form-filling $T_{\rm marg}/T_{\rm fff} \ll 1$. This highlights the paramount importance of finding efficient form-filling functions such as Chebyshev polynomials, we investigate the efficiency of Chebyshev, Fourier and top-hat basis sets in Appendix B.

We take random realizations of the coefficient space to uniformly sample the coefficients' possible values. This is a first, brute-force attempt at the problem. Alternative approaches could explore a set grid of values in this space, or use a more sophisticated random search such as a Monte Carlo chain approach – we leave this for future work.

In this first investigation, we have taken a simplistic approach and, as shown in Appendix B, we have found that a set of simple uniform random realizations is sufficient to explore the full space of functions.

Bayesian versus frequentist. One may be concerned that what we are advocating is a frequenist solution to the systematic problem. On contrary what we suggest is explicitly Bayesian: the method can take into account any prior information on the systematic from either theory or data. The specific method used in this article to find the form-filling functions is analogous to a brute-force parameter in maximum-likelihood reconstruction.

APPENDIX D: EXTREMAL OF THE BIAS

Here, we will show that given a hard boundary or some data there exists a maximum absolute bias. Within the Fisher matrix formalism, the bias caused by a function can be written (equation 12) as

$$b(\theta_i) = (F^{-1})_{ij} \sum s_C^{-2} C^{\rm sys} \frac{\partial C^{\rm signal}}{\partial \theta_j} \tag{D1}$$

where s_C is the observed signal variance. We can rewrite this as

$$b_\mu = (F^{-1})_{\mu\nu} C_\alpha^{\rm sys} s_\alpha^{-2} D_{\alpha,\nu}, \tag{D2}$$

where $D_{\alpha,\nu} \equiv \frac{\partial C_\alpha^{\rm signal}}{\partial \theta_\nu}$; we compress this to

$$b_\mu = C_\alpha^{\rm sys} Q_{\alpha,\mu}, \tag{D3}$$

where $Q_{\alpha,\mu} = (F^{-1})_{\mu\nu} s_\alpha^{-2} D_{\alpha,\nu}$.

We have the additional constraint that we are considering the set of systematic functions $\{S\}$ that give the same weight

$$\sum_\alpha \sigma_\alpha^{-2} \left(C_\alpha^{\rm sys} - d_\alpha\right)^2 = A^2 = \text{constant} \tag{D4}$$

with respect to some data vector d_α. In this proof and throughout the article, we assume that there is at least some systematic information

at every data value in the signal. If there was no constraint at the position of some of the signal data values then the bias would be unbounded.

For the hard boundary there is a constraint that $[C^{\rm sys}(x)]^2 \leq A^2$ at all x – this is actually for a constant (flat) hard boundary for a variable boundary the $A \rightarrow {\rm A(x)}$.

So, to find the maximum bias we need to solve the following equation

$$\frac{\partial}{\partial C_\gamma^{\rm sys}} \left\{ C_\alpha^{\rm sys} Q_{\alpha,\mu} - \lambda \left(\sum_\alpha \sigma_\alpha^{-2} \left(C_\alpha^{\rm sys} - d_\alpha \right)^2 - A^2 \right) \right\} = 0, \quad \text{(D5)}$$

where λ is a Langrange multiplier. Solving this for fixed μ and all γ, we find that

$$C_\gamma^{\rm sys} = \frac{1}{2\lambda} \sigma_\gamma^2 Q_{\gamma,\mu} + d_\gamma. \quad \text{(D6)}$$

To determine the value of the Lagrange multiplier, we substitute this back into the constraint equation (D4) to get a quadratic in $(1/2\lambda)$

$$\left(\frac{1}{2\lambda}\right)^2 \left(\sum_\alpha \left(\sigma_\alpha^2 Q_{\alpha,\mu} \right)^2 \right) + \left(\frac{1}{2\lambda}\right) \left(\sum_\alpha (2\sigma_\alpha^2 Q_{\alpha,\mu} d_\alpha) \right) + \left(\sum_\alpha d_\alpha^2 - A^2 \right) = 0. \quad \text{(D7)}$$

This has solutions of the form

$$\left(\frac{1}{2\lambda}\right) = R_\mu \pm T_\mu, \quad \text{(D8)}$$

where

$$R_\mu = -\frac{\left(\sum_\alpha 2\sigma_\alpha^2 Q_{\alpha,\mu} d_\alpha\right)}{2\sum_\alpha \left(\sigma_\alpha^2 Q_{\alpha,\mu}\right)^2}$$

$$T_\mu = \frac{\sqrt{\left(\sum_\alpha \sigma_\alpha^2 Q_{\alpha,\mu} d_\alpha\right)^2 - 4\left[\sum_\alpha \left(\sigma_\alpha^2 Q_{\alpha,\mu}\right)^2 \left(\sum_\alpha d_\alpha^2 - A^2\right)\right]}}{2\sum_\alpha \left(\sigma_\alpha^2 Q_{\alpha,\mu}\right)^2}. \quad \text{(D9)}$$

So, the function(s) with the maximum bias can be expressed as

$$C_\gamma^{\rm sys} = (R_\mu \pm T_\mu)\sigma_\gamma^2 Q_{\gamma,\mu} + d_\gamma. \quad \text{(D10)}$$

Note that there exists two functions that represent the maximum and minimum biases, which are given by

$$\max/\min(b_\mu) = \left[R_\mu \sigma_\alpha^2 Q_{\alpha,\mu} + d_\alpha\right] Q_{\alpha,\mu} \pm \left[T_\mu \sigma_\alpha^2 Q_{\alpha,\mu}\right] Q_{\alpha,\mu}. \quad \text{(D11)}$$

So, for a set of systematic functions that give the same weight with respect to some data there should exists a maximum and a minimum bias. Equation (D4) can be understood by looking at Fig. 7. For the data boundary case, there will be some large and small biases – actually every bias is 'allowed' but has some probability with respect to the data. Equation (D4) effectively takes a horizontal cut across on of the scatter plot panels in Fig. 7 at a given weight so that equation (D11) gives the minimum and maximum biases for that weight.

If the mean of the data is zero $\langle d_\alpha \rangle = 0$ and the variance of the data is $\langle d_\alpha^2 \rangle = \sigma_d^2$ then $\langle R_\mu \rangle = 0$ and

$$\langle T_\mu \rangle = \frac{\sqrt{A^2 - \sigma_d^2}}{\left[\sum_\alpha \left(\sigma_\alpha^2 Q_{\alpha,\mu}\right)^2\right]^{\frac{1}{2}}}, \quad \text{(D12)}$$

so that the mean bias is zero and the bias contours (contours are drawn for a constant weights, A) can be written as

$$\langle b_\mu \rangle = \pm \langle T_\mu \rangle \sigma_\alpha^2 Q_{\alpha,\mu}^2. \quad \text{(D13)}$$

For a hard boundary, we have

$$R_\mu = 0$$

$$T_\mu = \frac{A}{\left[\sum_\alpha \left(Q_{\alpha,\mu}\right)^2\right]^{\frac{1}{2}}} = A' \quad \text{(D14)}$$

which gives solutions for the maximum bias

$$\max/\min(b_\mu) = \pm A' Q_{\alpha,\mu}^2, \quad \text{(D15)}$$

this calculation can be compared to equations (D12) and (D13). This confirms that in the hard boundary case the absolute value of the bias has a maximum and that there exists two mirrored functions $[f(x)$ and $-f(x)]$ which both yield this maximum absolute bias.

In the case when the systematic is constrained by some data points $C^s ys_\alpha$, we can easily construct a function that goes through all the systematic data points but has unbounded 'bad effects' at some other point. However such a function, that has the same fit to the data but some other behaviour between the points is also assessed in terms of its impact on the cosmological parameter in question. Looking at Fig. 7 such a function would have the same weight but would have a smaller bias than a 'good function' that went through the same data points because the a_0 behaviour is not strongly degenerate with some 'bad behaviour' but has a simple functional dependency.

The key conclusion of this Appendix is that out of the space of all functions that have the same weight with respect to the data there exists a maximum and a minimum bias that this space of functions can cause.

APPENDIX E: DATA WEIGHTING

We know that given some error bars on data, and a different realization of the experiment, that the actual data points would be scattered differently but the statistical spread of the data would be the same. If a line fits *exactly* through some data points it is given a likelihood of exactly 1 but we know that this probability is spurious since given another realization of the experiment the data would be differently scattered and a new function would be assigned a probability of 1. This is a problem because $P = 1$ should be unique. This problem occurs because in the original step the probability of the data has not been taken into account.

For the specific Gaussian case, only we have used the marginalization over the probability of the data can be done analytically. We stress here that in general the systematic mean will be non-zero and that *only* in this very simplified Gaussian case (and some other analytic examples) can this procedure can be done analytically.

Here, we will outline how this 'sample variance effect' – that of taking into account the likelihood of the systematic data – can be incorporated into the χ^2-weighting scheme given in equation (26).

We can write the probability of a function $f[\boldsymbol{a}]$ as the sum over the data vector d_i multiplied by some prior probability of the data values $p(d_i)$

$$p(f[\boldsymbol{a}]) = \prod_i p(f_i|d_i)p(d_i), \quad \text{(E1)}$$

where $f_i = f(x_i, \boldsymbol{a})$ are the function values are the variable positions x_i at which the data has been taken.

We now want to marginalize over the probability of each data point to obtain $p(f[\boldsymbol{a}])$

$$p(f[\boldsymbol{a}]) = \int p(f[\boldsymbol{a}]|D){\rm d}D = \prod_i \int p(f_i|d_i)p(d_i){\rm d}d_i. \quad \text{(E2)}$$

Since we assume Gaussian data throughout the probability of the data can be written as a Gaussian centred about zero and $p(d_i|f_i)$ can be replaced with a χ^2 distribution such that

$$p(f[\boldsymbol{a}]) \propto \prod_i \int_{-\infty}^{+\infty} \mathrm{e}^{-\frac{(d_i-f_i)^2}{2\sigma_i^2}} \mathrm{e}^{-\frac{d_i^2}{2\sigma_D^2}} \mathrm{d}d_i, \tag{E3}$$

where σ_i is the error on the ith data point and σ_D is the variance of data which we take to be $\sigma_D = \sigma_i$. Note that each data point could have a different error bar – we have made the assumption that the data at each point is Gaussian distributed not that all data points are the same (the integral is over d_i not over i). Evaluating the integral in equation (E3), we have (now using log-likelihood for clarity)

$$\ln[p(f[\boldsymbol{a}])] \propto -\sum_i \left(\frac{f_i^2}{4\sigma_i^2}\right) + \sum_i \ln(\sigma_i\sqrt{\pi}). \tag{E4}$$

So that in the case of Gaussian-distributed data the probability of each function (and hence the probability of the bias incurred by that function) can be simply evaluated using equation (E4). Note that a Gaussian with a mean of zero is uniquely defined by its variance hence the data values themselves do not appear in the weighting formula given.

APPENDIX F: ICOSMO MODULE DESCRIPTION

The 'worst bias' calculations presented in Section 5 were done using an extension to the open source interactive cosmology calculator ICOSMO (Refregier et al. 2008b; Kitching et al. 2008d; http://www.icosmo.org). This additional module will be included in v1.2 and later.

The tomographic lensing module MK_BIAS_CHEB takes m_0 and β defined in equation (37) and uses the functional form-filling technique (using the Chebyshev basis set) to calculate the maximum bias in each cosmological parameter. The lensing survey and central cosmology can be arbitrarily defined using the common SET_FIDUCIAL routine described in Refregier et al. (2008b).

This paper has been typeset from a TEX/LATEX file prepared by the author.